GEOLOGICA CARPATHICA, JUNE 2009, 60, 3, 213–232 doi: 10.2478/v10096-009-0015-2

The Brodno section — a potential regional stratotype of the Jurassic/Cretaceous boundary (Western Carpathians)

JOZEF MICHALÍK[1], DANIELA REHÁKOVÁ[2], EVA HALÁSOVÁ[2] and OTÍLIA LINTNEROVÁ[3]

[1]Geological Institute of the Slovak Academy of Sciences, Dúbravská cesta 9, P.O.Box 106, 840 05 Bratislava 45, Slovak Republic; geolmich@savba.sk
[2]Department of Geology and Paleontology, Faculty of Natural Sciences, Comenius University, Mlynská dolina G-1, 842 15 Bratislava, Slovak Republic; rehakova@fns.uniba.sk; halasova@fns.uniba.sk
[3]Department of Economic Geology, Faculty of Natural Sciences, Comenius University, Mlynská dolina G-1, 842 15 Bratislava, Slovak Republic; lintnerova@fns.uniba.sk

(Manuscript received May 7, 2008; accepted in revised form October 23, 2008)

Abstract: Compared to coeval successions from the Carpathians, the continuous Jurassic-Cretaceous (J/K) pelagic limestone succession of the Brodno section offers the best possibility to document the J/K passage in a wide area. This section comprises a complete calpionellid, and nannofossil stratigraphic record, that supports the older paleomagnetic data. Moreover, the sequence stratigraphy and stable isotope ($\delta^{18}O$, $\delta^{13}C$) data gave important results, too, enabling comparison with known key sections from the Mediterranean Tethys area.

Key words: J/K boundary, Western Carpathians, regional stratotype, stable isotopes, biostratigraphy, microfossils, pelagic carbonates.

Geological context of the Brodno section: an overview

The Brodno section is situated in an abandoned quarry on the eastern side of the narrow straits of the Kysuca River Valley north of the town of Žilina (known as the "Kysuca Gate", Fig. 1). It yields a record of hemipelagic marine sedimentation in a marginal zone (the Pieniny Klippen Belt) of the Outer Western Carpathians. The lithology, fossil record (including ammonites and aptychi) and stratigraphy were studied by Andrusov (1938, 1950, 1959), Scheibner (1961, 1962, 1967), Borza (1969), Scheibner & Scheibnerová (1969), and Samuel et al. (1988). A more detailed description of the Upper Jurassic and Lower Cretaceous litho- and biostratigraphy was provided by Michalík et al. (1990), Reháková & Michalík (1992), and Vašíček et al. (1992). Houša et al. (1996) introduced the magnetostratigraphy of the Jurassic/Cretaceous (J/K) boundary beds correlated with the microbiostratigraphic data.

This paper discusses the results of an integrated biostratigraphic study using three microplankton groups (calpionellids, calcareous dinoflagellates and nannofossils), as well as stable isotope data ($\delta^{18}O$, $\delta^{13}C$) in the Brodno section, which is proposed here as the candidate for a West Carpathian regional J/K boundary stratotype. The distribution of the stratigraphically important planktonic organisms revealed several coeval calpionellid and nannofossil bioevents recorded in the pelagic carbonate sequence of the Jurassic/Cretaceous boundary age. The stable isotope data underline environmental changes during the interval studied.

According to the International Commission on Jurassic Stratigraphy, it is necessary to search for complete sections, which can provide continuous records of both sedimentation and biotic events across stage boundaries. Although the Brodno section lacks ammonite record, it is presented here as a potential candidate considering its continuously well exposed and biostratigraphically properly documented succession, at least for the West Carpathian region.

Material and methods

The Jurassic/Cretaceous boundary succession was studied using an integrated sequence-, bio- and isotope stratigraphy approach from the detailed rock section sampled. A quantitative microfacies analysis was carried in thin sections for the sequence stratigraphic pattern of these pelagic limestones (see Reháková 2000a; Michalík 2007). The calpionellids and calcareous dinoflagellates were studied under a light microscope LEICA DM 2500-P in 96 thin sections. They were documented by a LEICA DFC 290 HD camera. Thin sections are deposited in the Geological Institute of the SAS in Bratislava. Changes in the distribution of these organism remnants were studied aiming at their correlation with the nannoplankton associations.

The calcareous nannofossils were analysed in 40 smear slides prepared from all the lithologies under a light microscope at 1250× magnification. The abundance was determined by counting all the specimens in at least 200 fields of view in each sample. The preservation of the fossil material could be characterized by a moderate to heavy dissolution etching. The content of increased coccolite remnants in beds C13 and C23B is interpreted as due to diagenetic alteration of the calcareous nannofossils composition.

Carbon and oxygen isotope analyses were carried out on the bulk carbonate fraction in 52 samples from the J/K boundary interval in the Brodno section using a Finigan MAT-2 mass

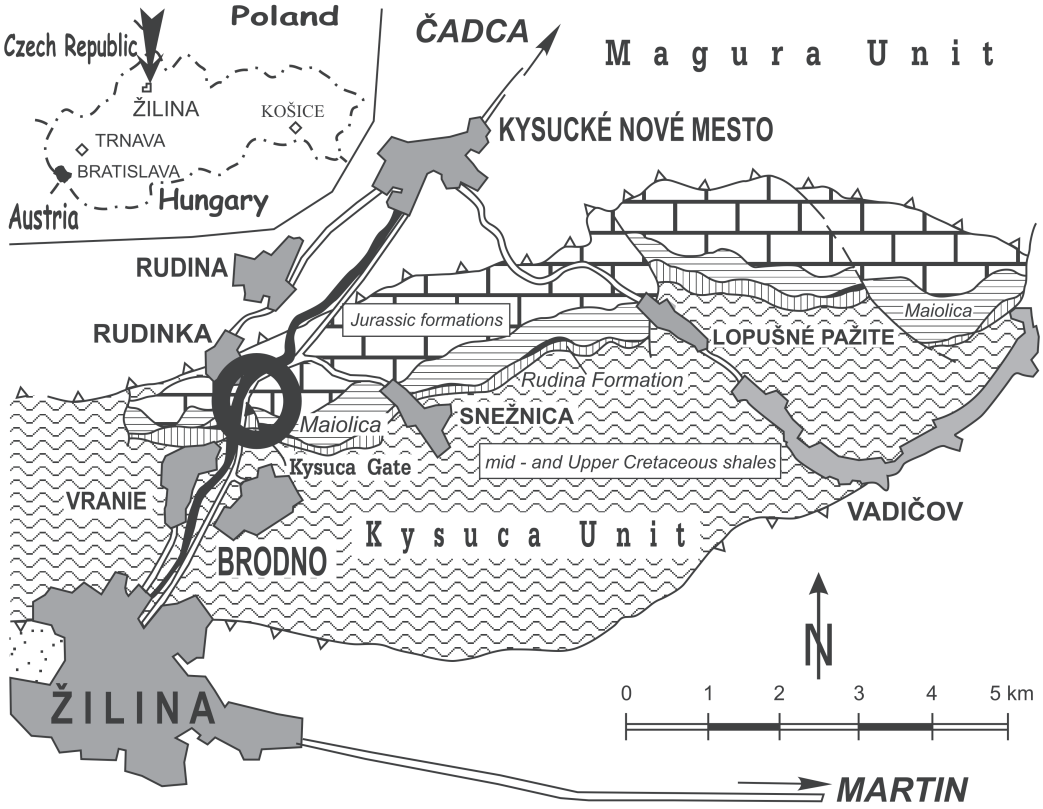

Fig. 1. Localization of the Brodno section in the Kysuca Gate (circle), north of Žilina.

Fig. 2. General view of the Brodno quarry. The sequence is overturned, the left upper side consists of the Czorsztyn Limestone Formation, and the right side is formed by the Pieniny Limestone Formation. Lower right: a detailed view of the interval of the Jurassic/Cretaceous boundary with the Brodno Sub-magnetochron.

spectrometer. The values are reported in terms of Vienna-PDB (V-PDB) in the standard δ notation in ‰, with a precision of 0.01 ‰. The total organic (TOC) and inorganic carbonate content (TIC) was measured on C-MAT 550. The paleotemperature calculation from calcite oxygen isotope (Epstein et al. 1953; Craig 1965; or Anderson & Arthur 1983) is as follows: paleotemperature (°C) = 16.0–4.14 $(\delta_c-\delta_w)+0.13\ (\delta_c-\delta_w)^2$. In this equation, the calcite oxygen isotope (δ_c) composition with respect to V-PDB is directly related to the oxygen isotope composition of seawater (δ_w) from which the calcite has precipitated with respect to V-SMOW. The value of –1.0 ‰ V-SMOW is characteristic of the post-Jurassic ice-free world (Gröcke et al. 2003). The TIC values were recalculated to the $CaCO_3$ content in order to assess the carbonate content of the samples selected for isotope analysis. A lot of the geochemical data have been presented previously (Michalík et al. 1995).

Results

Microbiostratigraphical remarks and reference scales

1. Calcareous dinoflagellate cysts. The distribution, abundance and diversity of calcareous dinoflagellate cysts is important both from the stratigraphical and paleoenvironmental points of view. Calcareous dinoflagellate cyst zonation sensu Reháková (2000b) was followed (Fig. 11). These biomarkers predominate in Lower Tithonian associations and are represented by: *Cadosina parvula* Nagy, *Stomiosphaera moluccana* Wanner — (Fig. 3.1), *Parastomiosphaera malmica* (Borza) — (Fig. 3.2), *Colomisphaera pulla* (Borza) — (Fig. 3.3), *Colomisphaera carpathica* (Borza) — (Fig. 3.4), *Colomisphaera nagyi* (Borza) — (Fig. 3.5), *Carpistomiosphaera tithonica* Nowak, *Cadosina semiradiata semiradiata* Wanner — (Fig. 3.6; Fig. 4.3), *Cadosina semiradiata*

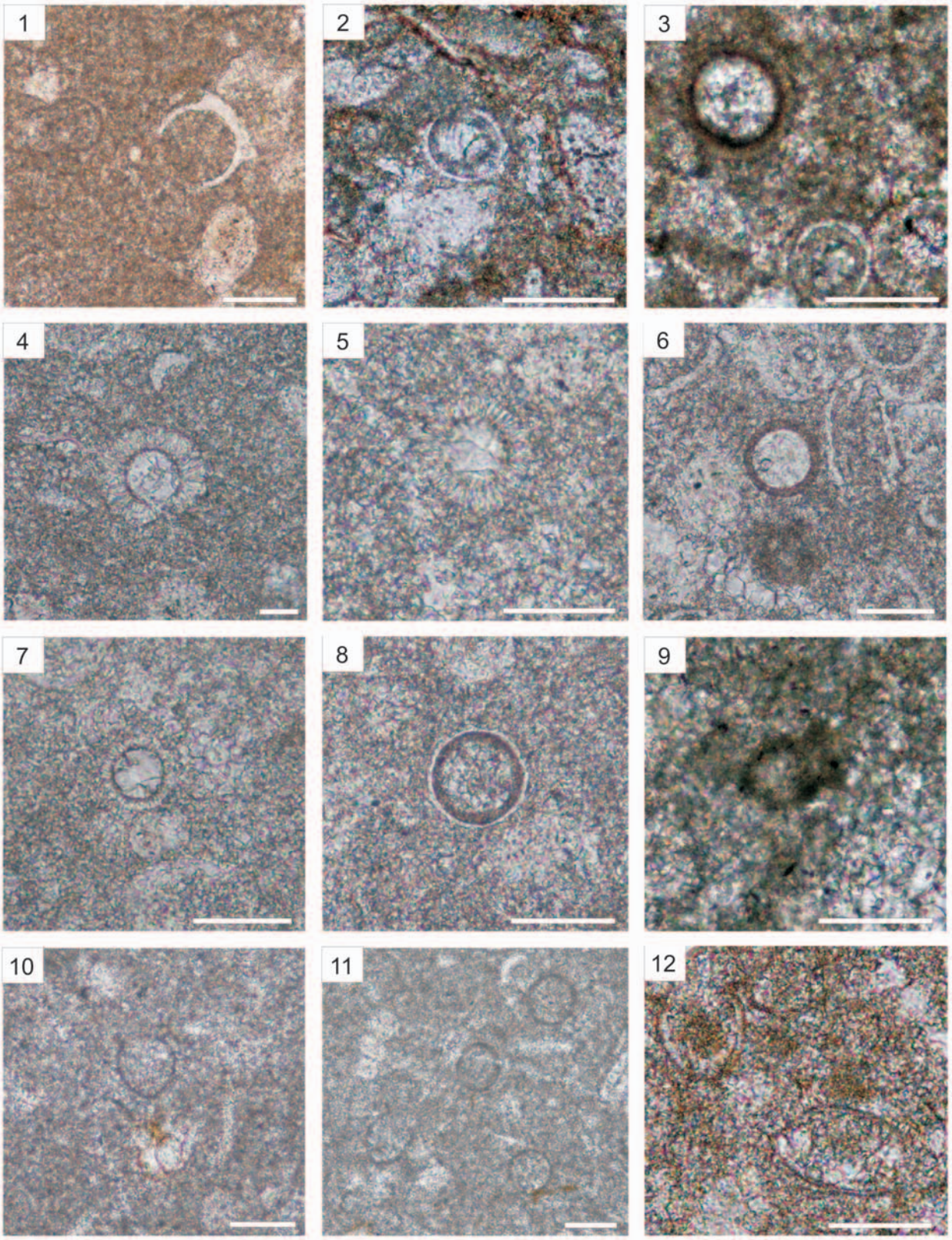

Fig. 3. Calcareous dinoflagellate cysts and early calpionellids: **1** — *Stomiosphaera moluccana* Wanner; Sample L51. **2** — *Parastomiosphaera malmica* (Borza); Sample L68. **3** — *Colomisphaera pulla* (Borza), *Parastomiosphaera malmica* (Borza); Sample L51. **4** — *Colomisphaera carpathica* (Borza); Sample L85. **5** — *Colomisphaera nagyi* (Borza); Sample L 83. **6** — *Cadosina semiradiata semiradiata* Wanner; Sample L87. **7** — *Colomisphaera tenuis* (Nagy); Sample L83. **8** — *Stomiosphaerina proxima* Řehánek; Sample C8/C. **9** — *Dobeniella tithonica* (Borza); Sample L83. **10** — *Borziella slovenica* (Borza); Sample L75. **11** — Microfacies with *Chitinoidella*; Sample L89. **12** — *Praetintinnopsella andrusovi* Borza; Sample L94. Light microscope Olympus BX 51 with Leica DFC 290 digital camera. Scale bar = 50 μm.

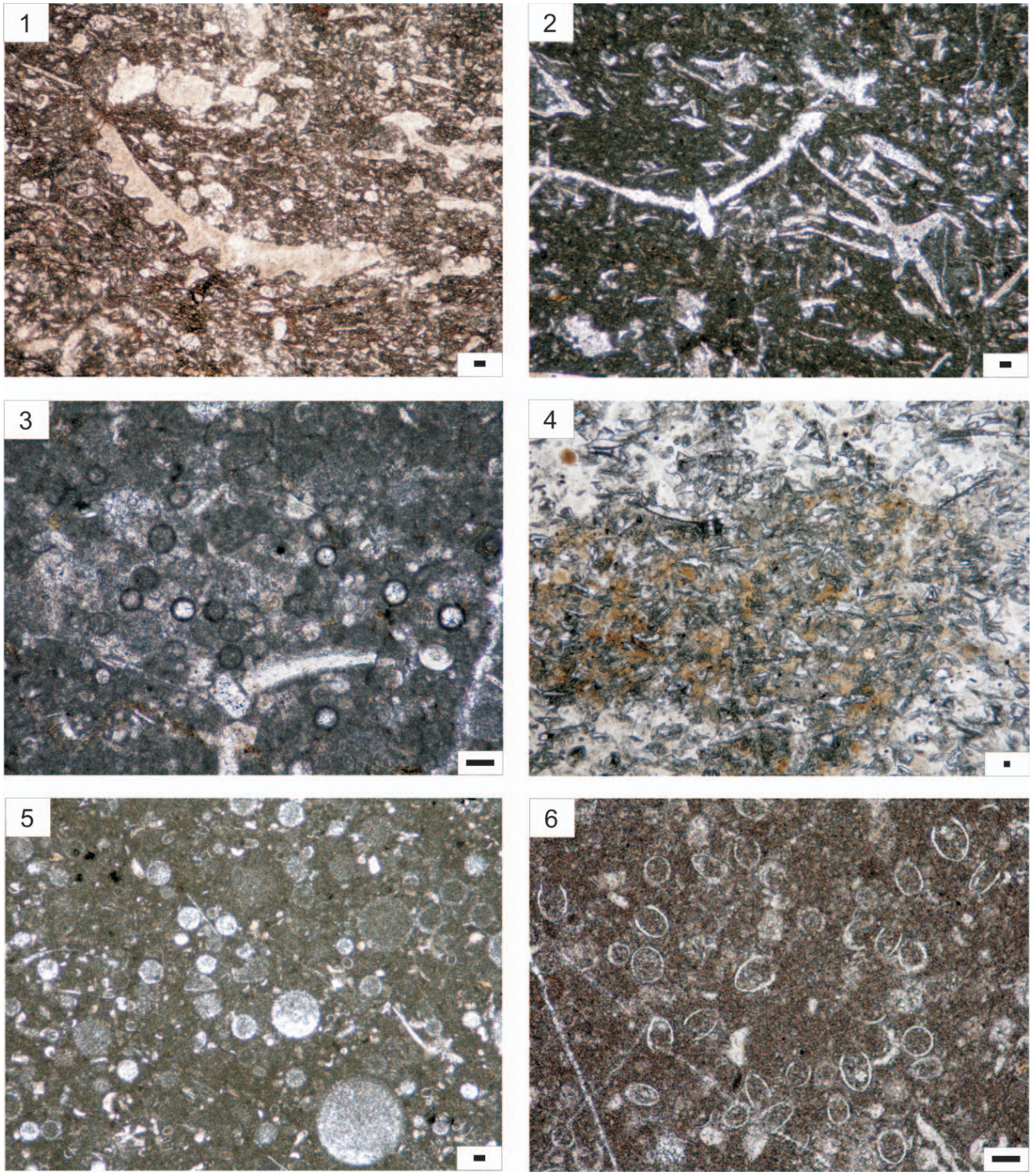

Fig. 4. Microfacies: **1** — *Saccocoma–Globochaete* microfacies with aptychi fragments; pale greenish to rosa-coloured limestones; Sample L51. **2** — *Saccocoma* microfacies; pale greenish to rosa-coloured limestones; Sample L58. **3** — Acme of *Cadosina semiradiata semiradiata* Wanner; pale rose-grey marly nodular to brecciated limestones; Sample L69. **4** — Silicified *Saccocoma* limestone; pale bedded indistinctly nodular biomicrite limestones; Sample L96. **5** — *Calpionella*-radiolarian microfacies; pale rose-grey "Maiolica" limestones; Sample C4/B. **6** — Abundant *Calpionella grandalpina* Nagy in *Calpionella* microfacies; pale rose-grey "Maiolica" limestones; Sample C6. Light microscope Olympus BX 51 with Leica DFC 290 digital camera. Scale bar = 100 μm.

fusca (Wanner), *Schizosphaerella minutissima* (Colom), *Colomisphaera tenuis* (Nagy) — (Fig. 3.7) and *Stomiosphaerina proxima* Řehánek (Fig. 3.8).

2. Calpionellids. From the mid-Tithonian, calpionellid associations appeared. In stratigraphical order, they consist of *Dobeniella tithonica* (Borza) — (Fig. 3.9), *Longicollaria dobeni*

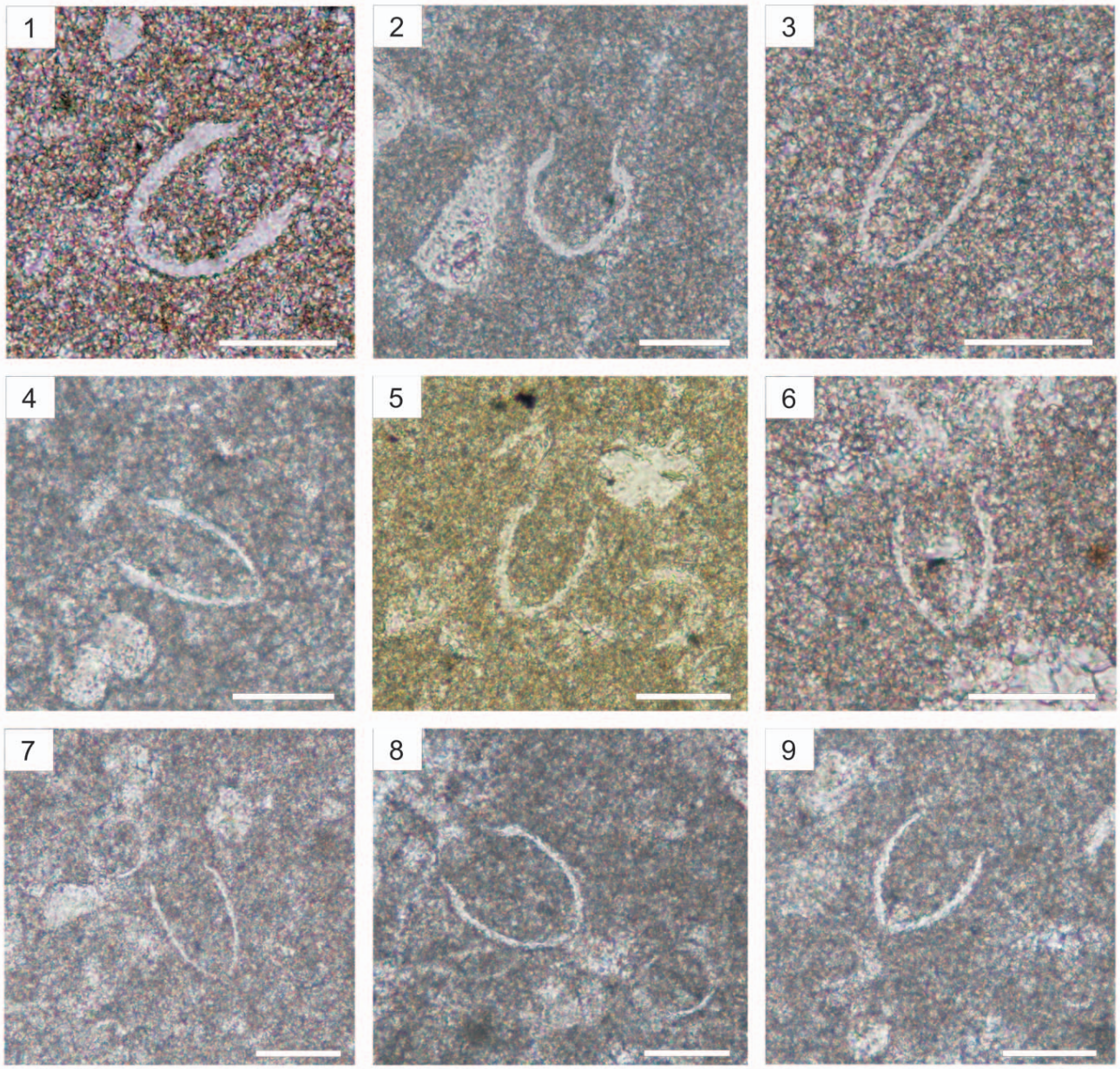

Fig. 5. Calpionellids: **1** — *Tintinnopsella remanei* Borza; Sample L99. **2** — *Calpionella alpina* Lorenz; Sample C3. **3** — *Crassicollaria intermedia* (Durand Delga); Sample L99. **4** — *Crassicollaria massutiniana* (Colom); Sample C3. **5** — *Crassicollaria brevis* Remane; Sample C12. **6** — *Crassicollaria parvula* Remane; Sample C4/B. **7** — *Crassicollaria colomi* Doben; Sample C22. **8** — *Calpionella grandalpina* Nagy; Sample C7. **9** — *Tintinnopsella doliphormis* (Colom); Sample C 24/A. Light microscope Olympus BX 51 with Leica DFC 290 digital camera. Scale bar = 50 μm.

(Borza), *Borziella slovenica* (Borza) — (Fig. 3.10), *Daciella danubica* Pop, *Chitinoidella boneti* Doben, *Borziella slovenica* (Borza) — (Fig. 3.10, 11), *Dobeniella cubensis* (Furrazola-Bermudez), *Dobeniella bermudezi* (Furrazola-Bermudez), *Tintinnopsella remanei* Borza — (Fig. 5.1), *Calpionella alpina* Lorenz — (Fig. 5.2), *Crassicollaria intermedia* (Durand Delga) — (Fig. 5.3), *Crassicollaria massutiniana* (Colom) — (Fig. 5.4), *Crassicollaria brevis* Remane — (Fig. 5.5), *Crassicollaria parvula* Remane — (Fig. 5.6), *Calpionella grandalpina* Nagy (Fig. 5.8), *Tintinnopsella carpathica* (Murgeanu & Filipescu), *Crassicollaria colomi* Doben (Fig. 5.7), *Tintinnopsella doliphormis* (Colom) — (Fig. 5.9) and *Remaniella ferasini* (Catalano). The preservation of the calpionellids is generally good. Their quantitative representation is variable, from less frequent in the case of chitinoidellids to abundant in the hyaline forms of calpionellids. Although the chitinoidellids are not perfectly preserved, they enabled the application of Pop (1997) and Reháková (2002) taxonomy. This study allows recognition of the Dobeni Subzone in the framework of the Chitinoidella Zone, not recorded in the Brodno section yet. The standard calpionellid zones and subzones, as proposed by Alleman et al. (1971), were adopted in the Western Car-

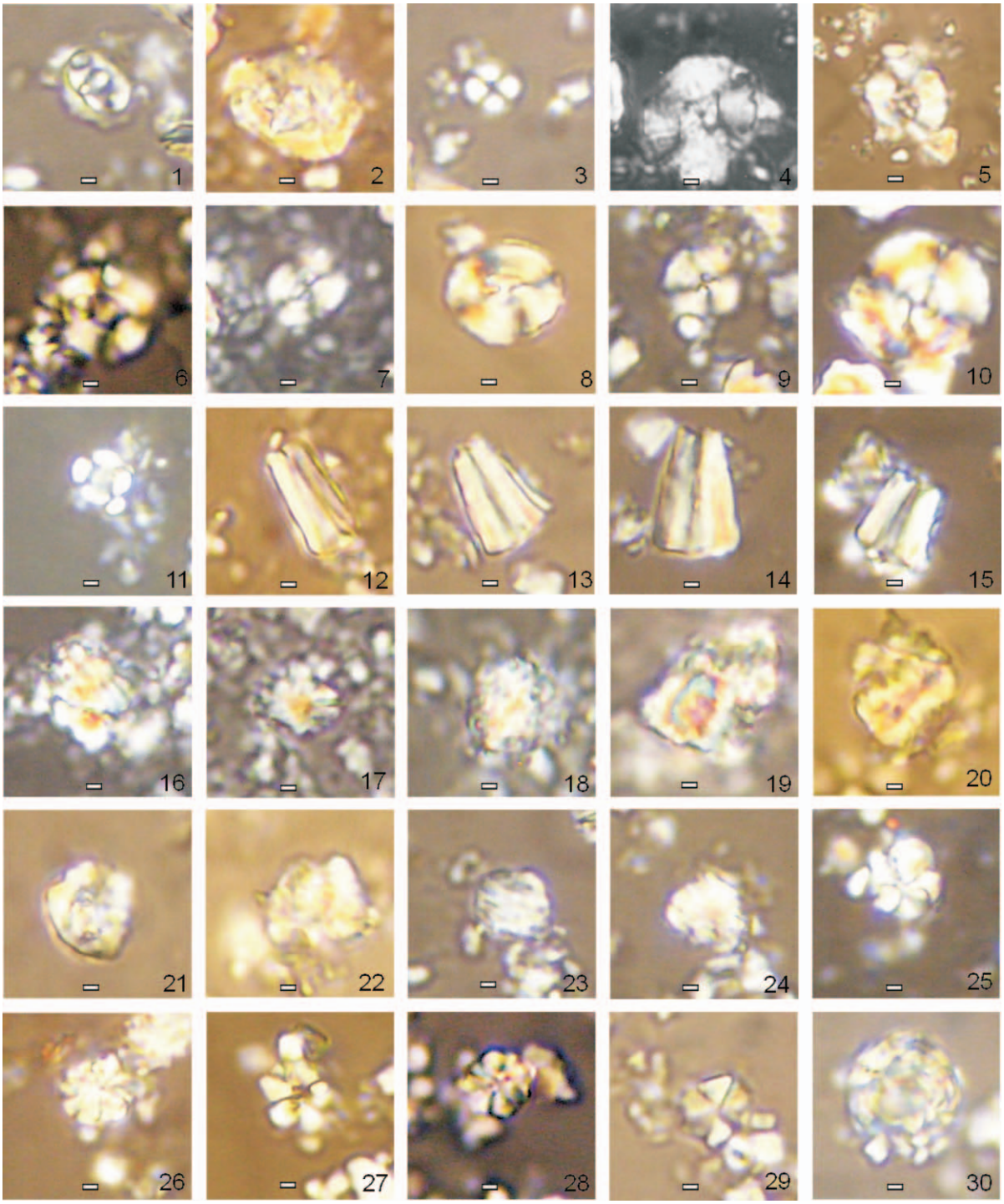

Fig. 6. Calcareous nannofossils: **1** — *Zeugrhabdotus erectus* (Deflandre) Reinhardt; Sample C4a. **2** — *Zeugrhabdotus embergeri* (Noël) Perch-Nielsen; sample L79. **3** — *Discorhabdus ignotus* (Górka) Perch-Nielsen; Sample C20. **4** — *Cruciellipsis cuvillieri* (Manivit) Thierstein; Sample C20. **5** — *Helenea chiastia* Worsley; Sample L98. **6** — *Watznaueria britannica* (Stradner) Reinhardt; Sample C20. **7** — *Watznaueria barnesae* (Black) Perch-Nielsen; Sample C24B. **8** — *Watznaueria manivitae* Bukry; Sample C25B. **9** — *Cyclagelosphaera margerelii* Noël; Sample C20. **10** — *Cyclagelosphaera deflandrei* (Manivit) Roth; Sample C17. **11** — *Diazomatholithus lehmannii* Noël; Sample C8a. **12–14** — *Conusphaera mexicana* Trejo subsp. *mexicana* Bralower et al. ; 12, 13 — C20,14 — C23B. **15** — *Conusphaera mexicana* Trejo subsp. *minor* Bown & Cooper; Sample C23D. **16–17** — *Nannoconus globulus* Brönnimann ssp. *minor* Bralower in Bralower et al., 1989; Sample C28. **18** — *Nannoconus steinmanni* Kamptner subsp. *minor* Deres & Achéritéquy; Sample C28. **19–20** — *Nannoconus kamptneri* Brönnimann subsp. *minor* Bralower in Bralower et al.; Sample C28. **21–22** — *Nannoconus wintereri* Bralower & Thierstein in Bralower et al.; Sample C17, C23D. **23–24** —*Nannoconus infans* Bralower; Sample C13, C20. **25–28** — *Polycostella beckmannii* Thierstein; Sample 25, 26 — L79; 27 — L77; 28 — L83. **29** — *Hexalithus noeliae* Loeblich & Tappan; Sample C8a. **30** — An unidentified coccosphaere; Sample C24A. Light micrographs by Olympus CAMEDIA digital camera C-4000 Zoom. Scale bar = 1 μm.

pathians by Borza (1984), Reháková (1995), and Reháková & Michalík (1997a). These references are also considered in this paper (Fig. 11).

3. Calcareous nannofossils form relatively low diversified associations. Eighteen nannofossil species have been determined in our sample collection. The coccolitophorids are represented by Watznaueriaceae including *Watznaueria barnesae* (Black) Perch-Nielsen (Fig. 6.7), *Watznaueria britannica* (Stradner) Reinhardt (Fig. 6.6), *Watznaueria manivitae* Bukry (Fig. 6.8), *Watznaueria ovata* Bukry, *Cyclagelosphaera margerelii* Noël (Fig. 6.9), and *Cyclagelosphaera deflandrei* (Manivit) Roth (Fig. 6.10). *Zeugrhabdotus embergeri* (Noël) Perch-Nielsen (Fig. 6.2) is another frequent constituent. Dissolution-resistant coccolith taxa *Helenea chiastia* Worsley (Fig. 6.5), *Cruciellipsis cuvillieri* (Manivit) Thierstein (Fig. 6.4) dominate among others, such as *Zeugrhabdotus erectus* (Deflandre) Reinhardt (Fig. 6.1), *Diazomatholithus lehmannii* Noël (Fig. 6.11), and *Discorhabdus ignotus* (Górka) Perch-Nielsen (Fig. 6.3). The last group is indicative of eutrophic environments, and occurs less frequently. Nannoliths represented by *Conusphaera mexicana* Trejo subsp. *mexicana* Bralower et al. (Fig. 6.12–14), C*onusphaera mexicana* Trejo subsp. *minor* Bown & Cooper (Fig. 6.15), *Polycostella beckmannii* Thierstein (Fig. 6.25–28), *Assipetra* spp., *Hexalithus noeliae* Loeblich & Tappan (Fig. 6.29), *Litraphidites carniolensis* Deflandre, *Nannoconus infans* Bralower (Fig. 6.23–24), *Nannoconus wintereri* Bralower & Thierstein in Bralower et al. (Fig. 6.21–22), *Nannoconus steinmanni minor* Deres & Achéritéquy (Fig. 6.18), *Nannoconus globulus* Brönnimann ssp. *minor* Bralower in Bralower et al. (Fig. 6.16–17), and *Nannoconus kamptneri minor* Bralower in Bralower et al. (Fig. 6.19–20) are abundant. Abundance fluctuation of dissolution-resistant nannoliths (*Conusphaera* spp., *Polycostella* spp., and *Nannoconus* spp.) and that of coccoliths (*Cyclagelosphaera margerelii*, *Watznaueria barnesae*, and *Watznaueria manivitae)* has been detected by quantitative analysis. The nannofossil zonations of Bralower et al. (1989), and Tavera et al. (1994), was used and slightly modified (Fig. 11).

Sequence stratigraphy and biostratigraphy

The succession starts with red nodular marly limestones of the "Ammonitico Rosso" lithofacies, known as the Czorsztyn Limestone Formation (Birkenmajer 1977). According to an analysis of the microfacies distribution (see Michalík 2007), several cyclical repetitions of the microfacies parameters were recognized in part of the sequence appearing on the left side of the quarry wall (Figs. 2, 7). These cycles are 0.5 to 1.6 m thick. Considering an average sedimentary rate of 2 mm/kyr, which results from microbiostratigraphical analysis of the formation, their duration should be roughly equal to 400 kilo-years (800 or 2400 kyr, respectively). As phenomena proving the condensation and amalgamation of cycles are generally common in this facies, these oscillations evidently had the character of Milankovich long eccentricity cycles. The architecture of these cycles seems to be controlled by eustatic sea-level changes. The sequence is arranged into inexpressive low frequency (40 kyr, i.e. obliquity) cycles expressed by an alternation of limestone layers and more marly insertions. The origin of these cycles was probably ruled by climatic (humidity driven) oscillations. The biostratigraphic boundaries are usually not identical with the sequence ones, the former usually running within the highstand part of the underlying cycle.

1. The lowermost **first cycle** is represented by beds L51 to L58 (Fig. 7). It consists of pale greenish to rosa-coloured limestones (*Saccocoma* to *Globochaete* wackestones, Fig. 4.1) with microfossils (*Cadosina parvula*, *Stomiosphaera moluccana*, *Cadosina semiradiata semiradiata*, *Colomisphaera pulla*, and *Carpistomiosphaera tithonica*) documenting Early Tithonian Pulla and Tithonica Zones. The last, thickest and most micritic layer (L58, Fig. 4.2) represents the highstand conditions close to the end of the M22 normal paleomagnetic Chron distinguished by Houša et al. (1996, 1999).

2. The **second cycle** is composed of thin-bedded nodular to brecciated pale greenish limestones (wackestone to packstone) with red cherts and marly interlaminae (L59 to L67 beds). The thicker L68 layer forms the highstand part of the cycle. In microfacies, *Saccocoma* Agassiz and *Globochaete alpina* Lombard predominate over crinoid ossicles, bivalve and aptychi fragments, ostracod shells, foraminiferal tests, calcified radiolarians, and dinoflagellates (*Cadosina semiradiata semiradiata*, *Cadosina semiradiata fusca* and *Parastomiosphaera malmica*). The last mentioned dinocysts represent an index association of the Early Tithonian Malmica Zone.

The calcareous nannofossil assemblage from the interval L52 to L68 (Fig. 5) is dominated by *Conusphaera mexicana mexicana*, *Conusphaera mexicana minor*, *Cyclagelosphaera margerelii*, *Cyclagelosphaera deflandrei*, *Watznaueria barnesae*, and *Watznaueria manivitae*. The absence of the nannolith *Polycostella beckmannii* in the association permits parallelization of this part of the sequence with the Early Tithonian Hexapodorhabdus cuvillieri (NJ 20-A) Subzone of the Conusphaera mexicana mexicana Zone (Roth et al. 1983; emended by Bralower et al. 1989).

3. Pale rose-grey marly nodular to brecciated limestones with red-brown cherts and red marly intercalations form the higher, **third cycle** (beds L69–L89).

3a. The lower part (beds L69–L74), which is correlatable with the upper part of the M21 normal Magnetozone, consists of radiolarian-globochaetid wackestone and packstone. The radiolarian tests are mostly calcified. Saccocomas occur frequently, and are accompanied by fragments of bivalve molluscs and aptychi, foraminiferal and ostracod tests. Acme accumulation of obliquipithonellid cadosinid thick-walled forms like *Cadosina semiradiata semiradiata* (L69, Fig. 4.3) and *Cadosina semiradiata fusca* (indicating the Semiradiata Acme Zone sensu Reháková 2000b) accompanied by abundant *Conusphaera* could be a proxy of increasing sea surface temperature conditions.

3b. The middle part (beds L75–L79) is formed by rose-grey biomicrite of the radiolarian-*Saccocoma-Globochaete* microfacies (packstone, wackestone). The

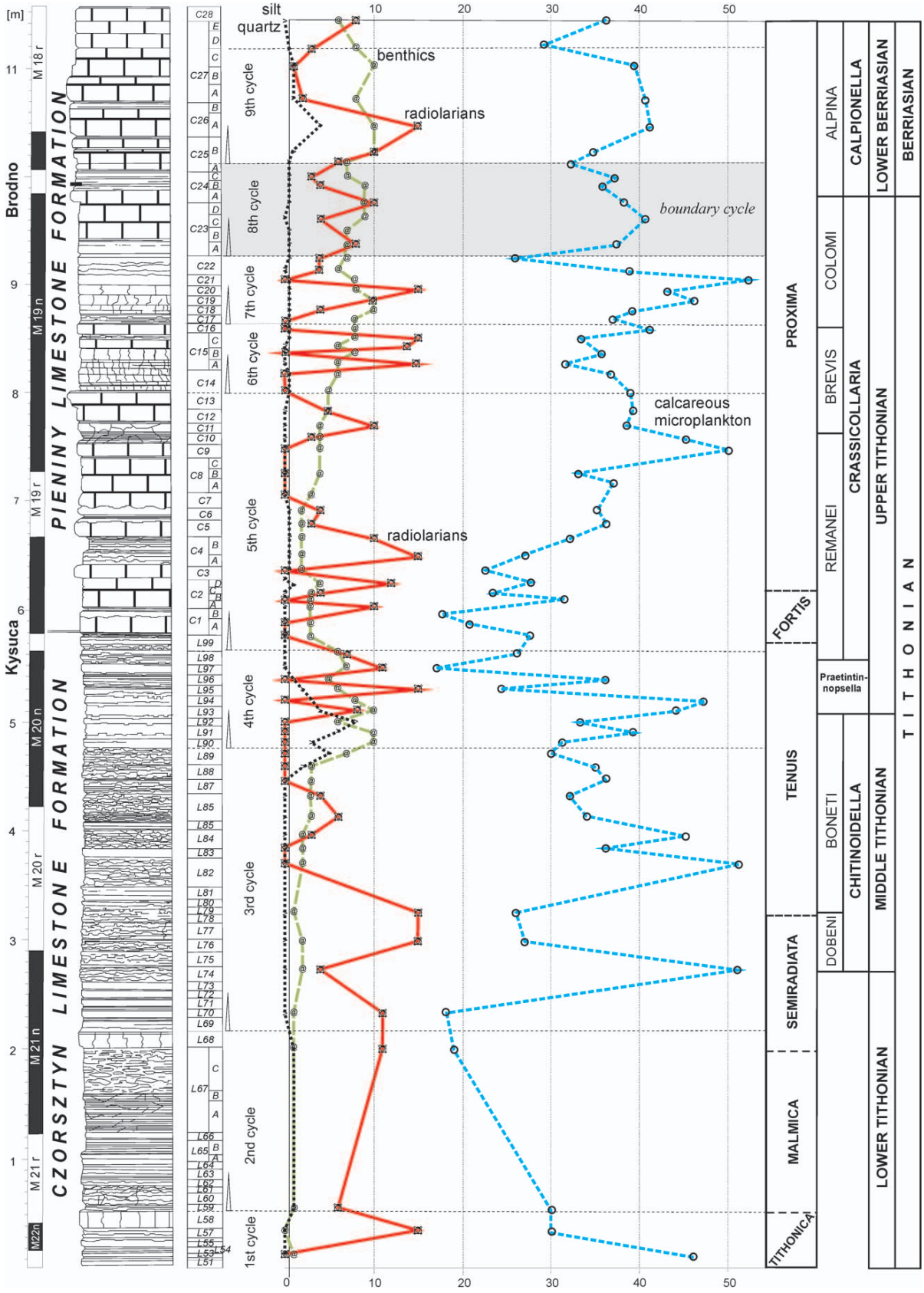

Fig. 7. Quantitative microfacies analysis of the Brodno section correlated with the magneto- (left side) and cycle stratigraphy (triangles indicate the base of cycles). The share of four principal allochem groups (silt quartz, clasts of benthic shells, radiolarian tests, tests of calcareous planktonic microorganisms) is shown in percents.

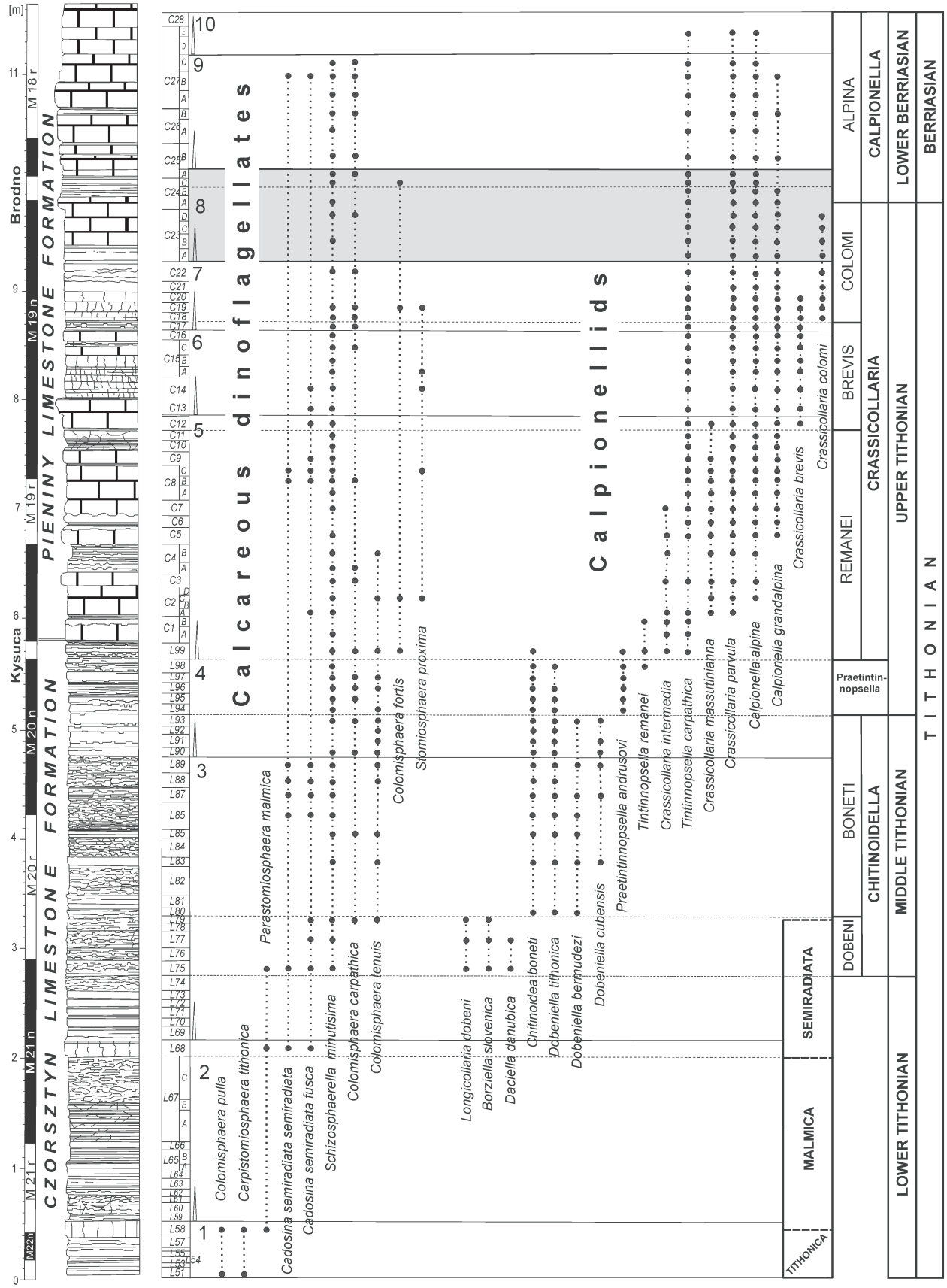

Fig. 8. Distribution of calpionellids and calcareous dinoflagellates (without quantitative aspect) in the Brodno section including combined calpionellid and dinoflagellate biozonation. Magnetostratigraphy and cyclostratigraphy shown for comparison on the left side.

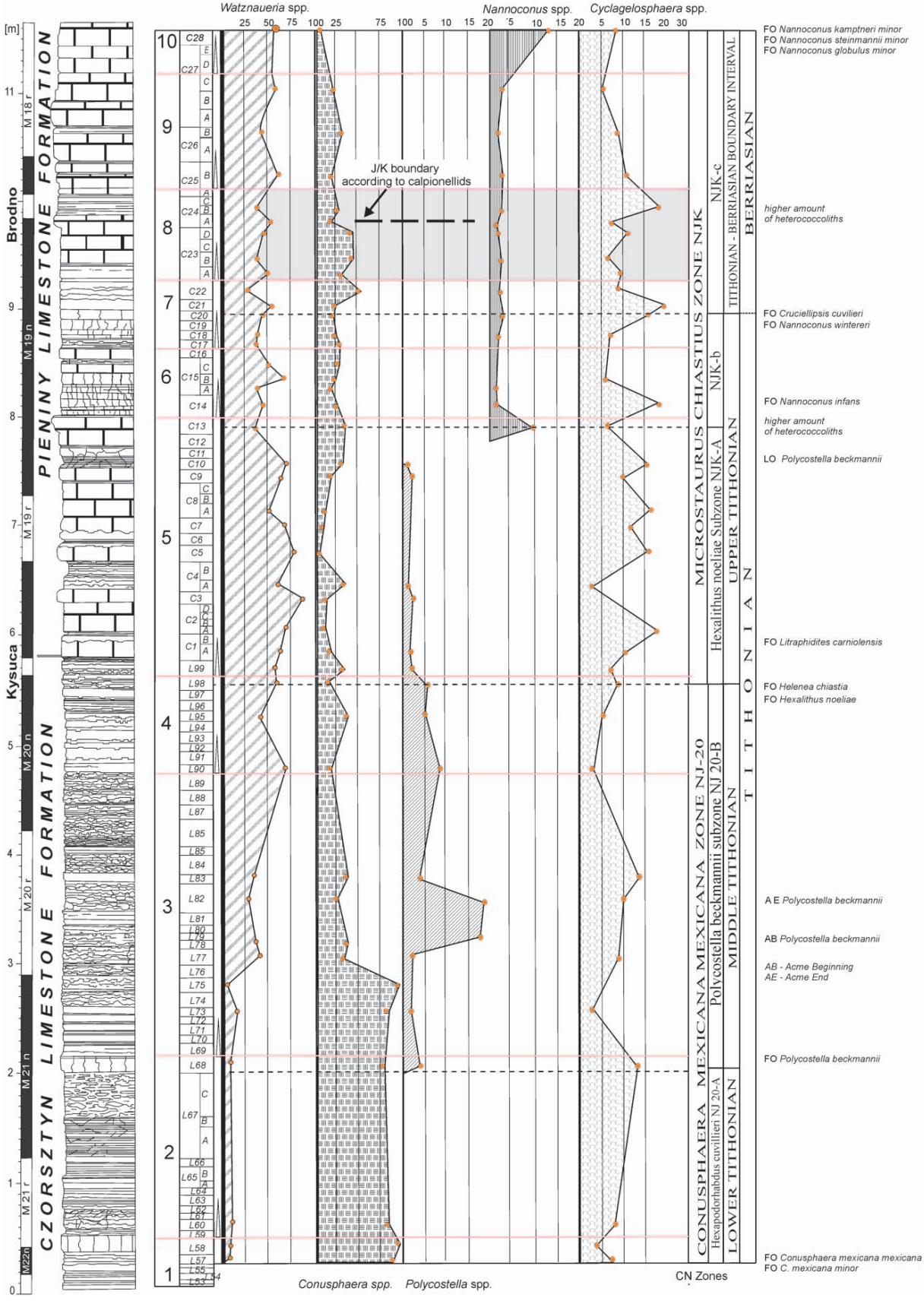

Fig. 9. Representation of nannoplankton abundance in the Brodno section including distinguished nannofossil zones and the main bioevents (first and last occurrences, maxima of abundance).

micrite matrix contains numerous calcified radiolarians, saccocomas and globochaetes. Bivalve fragments, juvenile ammonites and foraminifers (*Lenticulina* sp.) occur less frequently. Calcareous dinoflagellate cysts (*Parastomiosphaera malmica*, *Schizosphaerella minutissima*, *Colomisphaera carpathica*, *Cadosina semiradiata semiradiata*, *Cadosina semiradiata fusca*) and early calpionellid forms with microgranular lorica (*Longicollaria dobeni*, *Borziella slovenica* and *Daciella danubica*) indicate the Dobeni Subzone of the Middle Tithonian Chitinoidella Zone, which was distinguished in the Brodno section for the first time here. These strata are equivalent to the lowermost part of the M20 reversed Magnetozone (Houša et al. 1996, 1999).

3c. The upper part of the interval (L80–L89) consists of marly nodular to brecciated limestones with marly interlaminae. The calcareous content increases upwards up to thin bedded pale limestones with an indistinct nodular texture in the uppermost part. The rock microfacies and microfossil content is similar to that of the underlying beds. Calcareous dinoflagellates are represented by *Schizosphaerella minutissima*, *Colomisphaera carpathica*, *Colomisphaera nagyi*, *Colomisphaera tenuis*, and *Cadosina semiradiata semiradiata.* The occurrence of *Chitinoidella boneti*, *Borziella slovenica*, *Dobeniella tithonica*, *Dobeniella cubensis*, and *Dobeniella bermudezi* characterizes the Boneti Subzone of the Chitinoidella Zone.

Calcareous nannofossils obtained from L69 up to L96 were assigned to the Polycostella beckmannii Subzone (NJ 20-B; Roth et al. 1983; emended by Bralower et al. 1989) within the range of the Middle Tithonian; Magnetochron M21n to M20n (after Bralower et al. 1989). The assemblages of the lower part of this interval are typified by the predominance of *Conusphaera mexicana mexicana*, accompanied by *Conusphaera mexicana minor*, *Watznaueria barnesae,* and *Watznaueria manivitae*. The nannolitic form of *Polycostella beckmannii* reveals a high degree of abundance in the interval L77 to L83. *Discorhabdus ignotus* and *Zeugrhabdotus erectus* occur in a lower degree of abundance through this subzone.

4. The **fourth cycle** (L90–L98) is represented by a complex of pale bedded indistinctly nodular biomicrite limestones. Wackestones of radiolarian-*Saccocoma*-*Globochaete*, and locally silicified *Saccocoma*-radiolarian biomicrites (Fig. 4.4) contain mainly radiolarians, globochaetes, and saccocomids. Bivalve shell and aptychi fragments, ostracods, foraminifers, *Colomisphaera tenuis*, *Schizosphaerella minutissima*, and *Colomisphaera carpathica* are less frequent. Calpionellids *Chitinoidella boneti*, *Dobeniella tithonica*, *Dobeniella bermudezi* and transitional early hyaline forms of *Praetintinnopsella andrusovi* characterize the uppermost part of the Boneti Subzone (Chitinoidella Zone) and the passage into the Praetintinnopsella Zone.

5. The **fifth cycle** (Fig. 7) starts with the L99 layer, where the reverse paleomagnetic Kysuca Subzone has been distinguished by Houša et al. (1996) below a complex of well-bedded pale rose-grey "Maiolica" limestones of the Pieniny Limestone Formation (C1–C13). Limestone layers (4 to 20 cm thick) are separated by thin (2 to 40 mm) marly interlaminae. If the sedimentary rate is assumed to attain 2.9 mm/kyr (as deduced from the biostratigraphy), each a bed represents a time interval of up to 40 kyr. Cycles are then interpreted as climatically driven obliquity ones. A quantitative microfacies analysis indicates the presence of cyclical units (60 to 232 cm in thickness), which could represent eccentricity cycles. Biomicrite wackestone with *Crassicollaria-Globochaete*-radiolarian microfacies (Fig. 4.5) contains *Crassicollaria intermedia*, which predominate over *Crassicollaria massutiniana*, *Crassicollaria parvula*, *Calpionella alpina*, *Calpionella grandalpina* (Fig. 7.8), *Tintinnopsella remanei,* and *Tintinnopsella carpathica*. The association of calcareous dinoflagellates is composed of *Schizosphaerella minutissima*, *Colomisphaera carpathica*, *Cadosina semiradiata semiradiata*, *Cadosina semiradiata fusca*, and *Stomiosphaerina proxima* (an Early Berriasian age was attributed to the last mentioned cyst by Řehánek 1992, only). The calpionellid index association indicates the Remanei Subzone of the Crassicollaria Zone.

Samples L98 to C26 were attributed to the Microstaurus chiastius Zone NJK (Fig. 11) (sensu Bralower et al. 1989). In this work, the FO of *Helenea chiastia* and *Hexalithus noeliae* indicates the Late Tithonian Hexalithus noeliae Subzone (NJK-A). Coccoliths of the Watznaueriaceae group (*Watznaueria barnesae, Watznaueria manivitae*) fluctuate in a range from 25 to 80 %. The abundance of *Cyclagelosphaera margerelii* fluctuates in a range from 3–20 % in the whole succession. *Discorhabdus ignotus* and *Zeugrhabdotus erectus* occur in a higher degree of abundance (up to 10 %) in the C1B bed. The LO of *Polycostella beckmannii* observed in the C4A sample indicates a Late Tithonian age.

6. The **sixth cycle** (C14–C16) is built up of well bedded pale Maiolica limestones with thin (up to 2 cm) marly interbeds. *Crassicollaria-Globochaete* and radiolarian-*Crassicollaria* microfacies in biomicrite wackstone is dominated by globochaetes and calpionellids. A general decrease in calcareous plankton abundance is correlated with increase of radiolarians. Calpionellids are dominated by small forms of *Crassicollaria brevis. Calpionella grandalpina*, *Calpionella alpina*, *Crassicollaria parvula* and *Tintinnopsella carpathica*, saccocomas, radiolarians, aptychi, bivalve fragments and foraminifers (*Lenticulina* sp., *Spirillina* sp.) are rare. The association of calcareous dinoflagellates consists of *Schizosphaerella minutissima*, *Colomisphaera carpathica,* and *Stomiosphaerina proxima*. The interval was attributed to the Brevis Subzone of the Late Tithonian Crassicollaria Zone.

The FO of *Nannoconus infans* (C13) and the FO *Nannoconus wintereri* (C17) has been recorded in the interval with dominance of small crassicollarians. Both forms (according to Tavera et al. 1994) indicate the Late Tithonian NJK-b to NJK-c subzones. According to Tremolada et al. (2006), both these forms flourished under warmer and possibly more nutrient-depleted surface waters.

7. The **seventh cycle** — bedded pale grey limestone with thin (up to 2 cm) interbeds of marl (C17–C22) consists of biomicrite wackestone to packstone of crassicollarian-globochaete and radiolarian-globochaete-crassicollarian microfacies. *Globochaete* occurs commonly; *Crassicollaria parvula*

and *Calpionella grandalpina* predominate over *Crassicollaria colomi*. *Calpionella alpina*, *Tintinnopsella carpathica*, and *Tintinnopsella doliphormis* are frequent. The association of calcareous dinoflagellates contains *Schizosphaerella minutissima*, *Colomisphaera carpathica*, *Colomisphaera fortis*, and *Stomiosphaerina proxima*. The presence of *Crassicollaria colomi* indicates the Colomi Subzone of the Crassicollaria Zone. Sole *Cruciellipsis cuvillieri* was found in C20, close to the FO of *Nannoconus wintereri*. Bralower et al. (1989) correlated this datum with the base of the Calpionella alpina Zone coinciding with the top of the ammonite Durangites Zone.

8. The **eighth cycle** — well bedded pale grey biomicritic wackestone with thin (up to 1 cm) marly insertions (C23A–C25A). The calpionellid-globochaete microfacies is dominated by small sphaerical forms of the *Calpionella alpina*. Crassicollarians (*Crassicollaria parvula*, *Crassicollaria colomi*) along with *Calpionella grandalpina* and *Tintinnopsella carpathica* are less frequent. The base of the Alpina Subzone of the Calpionella Standard Zone was identified in the C24A Bed. The Brodno Magneto-Subchron was located in layer C24B.

9. The **nineth cycle** — well bedded pale biomicritic wackestones with *Calpionella-Globochaete* and *Calpionella*-radiolarians microfacies (C25B–C27E). As a rule, the degree of abundance of radiolarians is inversely related to that of calpionellids (Fig. 7; Reháková & Michalík 1994; Pszczółkowski et al. 2005). Limestones also contain frequent *Globochaete alpina*; foraminiferal fragments, radiolarians, ostracods, aptychi, ophiuroids, bivalves, juvenile ammonites, *Crassicollaria parvula*, *Tintinnopsella carpathica*, *Cadosina semiradiata fusca*, *Cadosina semiradiata semiradiata* are very rare. The microbreccia layers contain small limestone clasts with Tithonian microfossils.

10. The **tenth cycle** — a complex with anomalously thick (20–48 cm) layers of biomicritic *Calpionella* wackestone (C28A–C29A). Its upper part shows submarine slumping features. Small sphaerical forms of *Calpionella alpina* still dominate the calpionellid association. The FO of *Nannoconus steinmanni minor*, the increase in abundance and diversity of nannoconids in C28 enabled drawing the base of the NJK-D Nannoconus steinmanni subsp. minor Subzone, which is correlated with the lowermost Berriasian. The association of calcareous nannofossils in this part of the succession is characteristic of the start of the nannoconid bloom and the FO of *Nannoconus steinmanni minor*, *Nannoconus globulus minor*, and *Nannoconus kamptneri minor*. These forms are accompanied by *Conusphaera mexicana mexicana*, *Cyclagelosphaera deflandrei*, *Cyclagelosphaera margerelii*, *Diazomatholithus lehmannii*, *Discorhabdus ignotus*, *Watznaueria barnesae*, *Watznaueria britannica*, *Watznaueria manivitae*, and *Zeugrhabdotus embergeri*.

11. The **eleventh cycle** — thick-bedded cherty limestones with radiolarian-*Calpionella* microfacies (C29B–C38). Abundant radiolarians are dispersed in the wackestone, but also concentrated in six 4–6 cm thick radiolarite layers. The first occurrence of *Remaniella ferasini* (Catalano) in the overlying thick-bedded cherty "Maiolica" limestones indicates the base of the Ferasini Subzone of the standard Calpionella Zone (Reháková & Michalík 1997a).

Isotope geochemistry, chemostratigraphy

The C and O isotope ratios could have been influenced by burial history of sediment due to recrystallization of primary carbonate minerals, to cementation and temperature increase with burial depth, and to other processes. Fine-grained limestone composed mainly of calcitic micro- and nannoplankton tests could retain its primary character. The fossils could have been broken and disturbed, partially dissolved and recrystallized in micro-scale, but the carbonate composition still indicates low diagenetic overprint and its composition can be regarded as more-or-less primary. Carbon isotope curves from bulk carbonate samples of the J/K boundary sequences worldwide show smooth trends resulting from equilibrated rates of bio-productivity and organic matter burial (Weissert & Mohr 1986; Weissert & Channel 1989; Weissert & Lini 1991; Gröcke et al. 2003; Tremolada et al. 2006). In the Brodno sequence, the average value of $\delta^{13}C$ (L90–C27: 1.45 ‰) ranges between 1.3 and 1.5 ‰ (PDB) (Fig. 10).

The lowermost cycle (up to L58) as a part of the Czorsztyn Limestone Formation (the Ammonitico Rosso facies) contains slightly a rised $\delta^{13}C$ values (1.46–1.73 ‰). In the second, third and fourth cycles, $\delta^{13}C$ values gradually decrease to the lowest value in L98 (1.28 ‰). The only small positive excursion occurs in the L79 (1.51 ‰) sample, corresponding to the *Polycostella* peak. Rhythmic fluctuations during gradual rise of the average $\delta^{13}C$ values in the 4th to 6th cycle (start of the Maiolica facies at the base of the Pieniny Limestone Formation) probable reflect the rhythmic character of the rock sequence due to sea-level oscillations (Figs. 7,10). A much wider range of $\delta^{13}C$ values (1.55–1.33) is recorded from the 7th cycle (immediately below the J/K boundary level) with a decrease in their average. The $\delta^{13}C$ values increase again in the cycles above the J/K boundary.

The authentic character of the $\delta^{13}C$ record of our samples is underlined by relatively high and conservative $\delta^{18}O$ values (–2.29 to –0.88). The fractionation of oxygen isotopes is more sensitive to temperature and salinity variations in the marine water. The $\delta^{18}O$ values in carbonate rock could reflect these environmental proxies recorded by micro- and nannofossils (Price et al. 1998; Gröcke et al. 2003; Hay et al. 2006; Tremolada et al. 2006).

The mathematic average of the $\delta^{18}O$ value in the Brodno section attains –1.62 ‰. $\delta^{18}O$ values less than the average (from –1.85 to –2.29 ‰) in the 2nd cycle could reflect a relatively warmer episode during the Early Tithonian with temperature changes in the range of 2–3 °C (Fig. 6). Positive excursions in cycles 3 and 4 (approximately –1.5 ‰) indicate a progressive fall of temperature (nearly 2–3 °C), which is more or less correlatable with the *Polycostella* flowering (Fig. 9). A higher positive $\delta^{18}O$ excursion (C3 bed) potentially indicates a change other than a temperature fall only. This positive $\delta^{18}O$ event was accompanied not only by earlier diminishing of *Polycostella*, but also by drift of abundance of *Watznaueria* and *Cyclagelosphaera* which could indicate changes of water composition, for example of salinity or eutrophication. Around the J/K boundary (cycles 6, 7 and 8), the more negative $\delta^{18}O$ values (–1.5 to –2.6 ‰) indi-

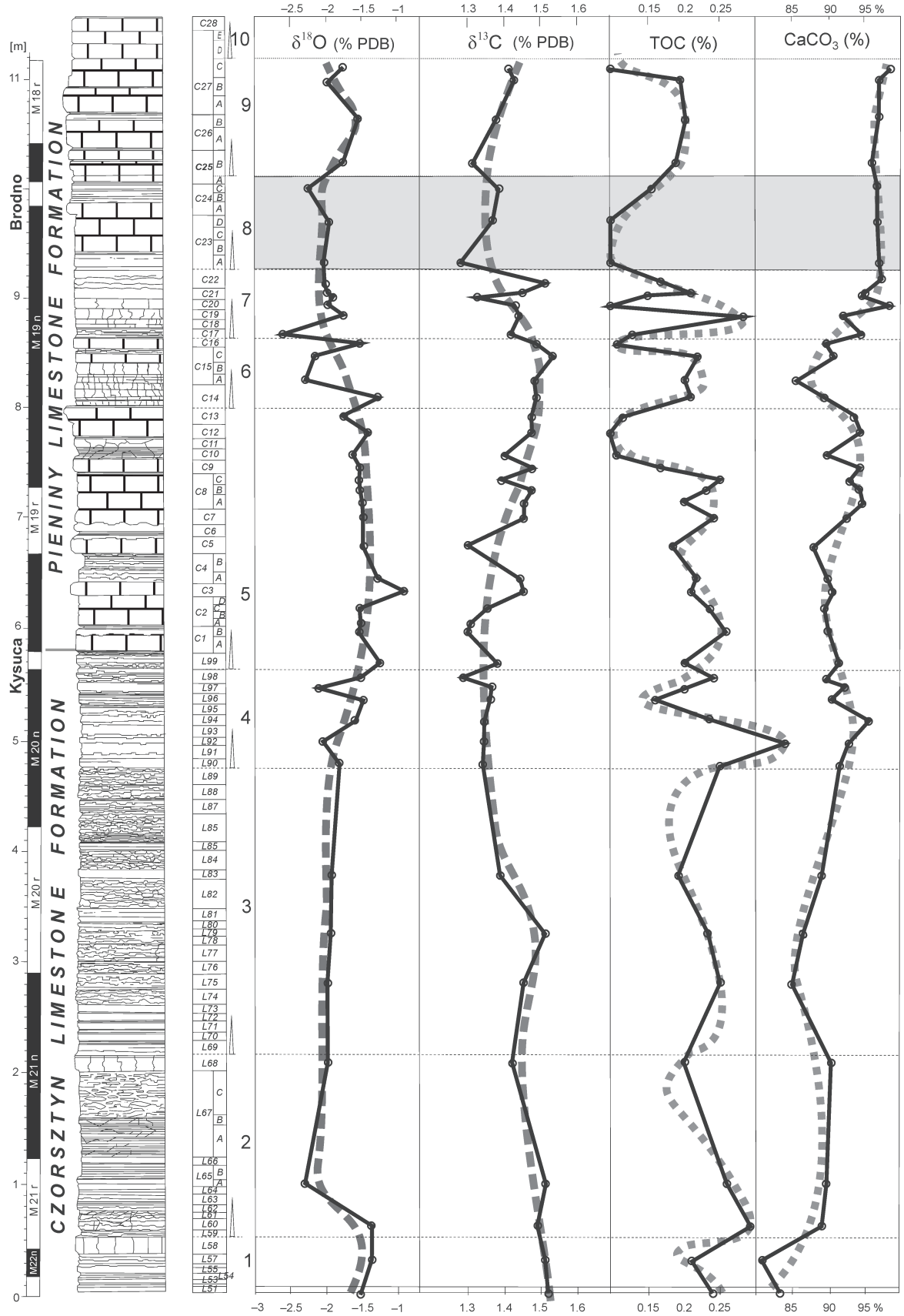

Fig. 10. Carbon and oxygen isotope data, total organic carbon and calcium carbonate content in the Brodno sequence correlated with magnetostratigraphy and cycle stratigraphy.

cated a temperature increase. This is also indicated by rich *Nannoconus* occurrence that pleads in favour of the end of the cold period. Stable isotope analyses also proved a modest cooling of the earliest Berriasian surface waters.

Organic matter contents in the Lower Tithonian 1st to 5th cycles (0.15 to 0.25 %) are gradually decreasing upwards in each cycle. This fluctuation could be related to changing humidity, which is also supported by rapid lithofacies fluctuations (Fig. 7). The most impressive peak was observed at the beginning of cycle 4 (L93; Fig. 6). The lowest values were attained just below the J/K boundary, in the upper parts of the cycles 5 to 8 (on the base of the Pieniny Limestone Formation). On the other hand, the calcium carbonate content is gradually increasing (from 85 to 97 %) with small minimum in cycle 6 at the base of the Pieniny Limestone Formation (Fig. 6). The carbonate content increase fits well with the onset of nannoconids.

Discussion

As in many other Tethyan areas, the Late Jurassic sedimentation rate in the Pieniny Klippen Basin was low. The condensed red nodular limestones of the "Ammonitico Rosso Facies" (the Czorsztyn Limestone Formation), which represent the Kimmeridgian and Tithonian part of the Kysuca Succession, received only a limited terrigenous clastic input. In an analysis of the periodicity of the Milankovitch frequency bands in the Spanish Rio Argos section, Hoedemaeker & Lereveld (1995) situated sequence boundaries at the base of marly interbeds. Similarly, according to Schlager (2005), siliciclastics may be found in all system tracts, as they are a common constituent of basinal lowstand fans ("reciprocal sedimentation"). To the contrary, Michalík (2007) argued that the character of lowstand deposits strongly depends on the lithological composition of the shore area that emerged. As the Lower Cretaceous lowstand sequences in the West Carpathian area were mostly supplied by carbonate platform-derived calcidetritus, they were formed by fine-detrital (the grain size depends on the proximity/distality trends) limestone beds.

During the Berriasian age, subsiding West Carpathian basins were characterized by a great acceleration in the "planktonic rain" of organic matter and calcareous microskeletons. This change, which was detectable in the majority of West Carpathian successions also produced pelagic sediments of the "Maiolica" type (the Pieniny Limestone Formation). This sedimentary pattern persisted until the Early Aptian in the Pieniny Klippen Belt (Michalík et al. 2008).

The J/K boundary line: a historical review

The J/K boundary has represented a source of controversy for several decades. The problem consists mainly in the difference of local facies in different regions of the world, the lack of ammonites with more than provincial distribution, and reliable index fossils (Borza 1984; Remane 1991; Ogg et al. 1991; Adatte et al. 1994). Four variants of the J/K boundary have been drawn until the present: 1) the base of the Durangites Zone, 2) the base of the Jacobi Zone, 3) the base of the Occitanica Zone, and 4) the base of the Beriasella privasensis Zone.

1. Houša et al. (1996) discussed identification of the J/K boundary with the base of the Durangites Zone, which should be identical with the marked calpionellid event — FO of *Calpionella grandalpina* Nagy (base of the Remanei Subzone inside the Crassicollaria Zone), which is approximately at the beginning of the M19r Magnetochron. This opinion has now been practically abandoned.

2. Long discussions about the placing of the J/K boundary (Flandrin et al. 1975; Remane et al. 1986) have been terminated by the recommendation (Hoedemaeker et al. 1993) to draw this line at the base of the Jacobi Zone. This datum line should be situated at the base of the Alpina Zone of calpionellids. Channel & Grandesso (1987) correlated the magnetostratigraphy of the Jurassic/Cretaceous boundary with micropaleontological proxies. They put the boundary between the Crassicollaria/Calpionella Zones, inside the M19n Magnetochron. Bralower et al. (1989) parallelized the FO's of *Cruciellipsis cuvillieri* and *Nannoconus wintereri* with the uppermost part of the Crassicollaria Zone (= uppermost Durangites Zone). However, Olóriz & Tavera (1990), Tavera et al. (1994), and Olóriz et al. (1995) placed the base of the Jacobi Zone within the Crassicollaria Zone (in the Jurassic/Cretaceous Ammonitico Rosso sequence of the Puerto Españo section) close to the A2/A3 boundary. They proposed a division of the NJK Zone (Fig. 11) based on the FO's of *Nannoconus infans*, *Nannoconus wintereri* and *Nannoconus steinmanni minor* with the designations NJK-b to NJK-d. Gradstein et al. (1995) dated this time level as 144.2± 2.6 Ma. According to Houša et al. (1999), the base of the standard Crassicollaria Zone in the Brodno section lies approximately in the middle of the M20n Magnetozone. The base of the standard Calpionella Zone, namely the Jurassic/Cretaceous boundary lies in the middle part of the M19n Magnetochron (his solution 2), between C15A and C15B beds. These authors correlated their Brodno section data with sections in northern Italy (Foza), central Italy (Val Bosso), and Spain (Rio Argos). Pszczółkowski et al. (2005) identified the NJK-c Subzone with the Late Tithonian Nannoconus wintereri Subzone. Grabowski & Pszczółkowski (2006) located the Jurassic/Cretaceous boundary (between the A and B calpionellid biozones of Remane 1971; Remane et al. 1986) within the M19n Magnetochron, below the Brodno (M19n-1r) Subchron.

3. Ogg & Lowrie (1986) put the J/K boundary at the base of the Grandis/Occitanica Zone (~top of the Jacobi Zone = the base of the Tirnovella subalpina Zone, correlated with the base of the M18r Magnetochron.

4. The interval immediately above the base of the Beriasella privasensis Zone (= M18n/M17r; Lowrie & Channel 1983; Márton 1986) is typical of a drowning event (Gawlick & Schlagintweit 2006), with synsedimentary slumpings (Hoedemaeker & Leereveld 1995), kaolinite- (Schyder et al. 2005), phosphate- (Houša et al. 2006b), or iridium enrichment (Zakharov et al. 1996), or even with the Mjølnir- (Dypvik et al. 2006), Shatsky Rise- and Morokweng impact craters (Koberl et al. 1997; Mahoney et al. 2005; Tremolada et al. 2006).

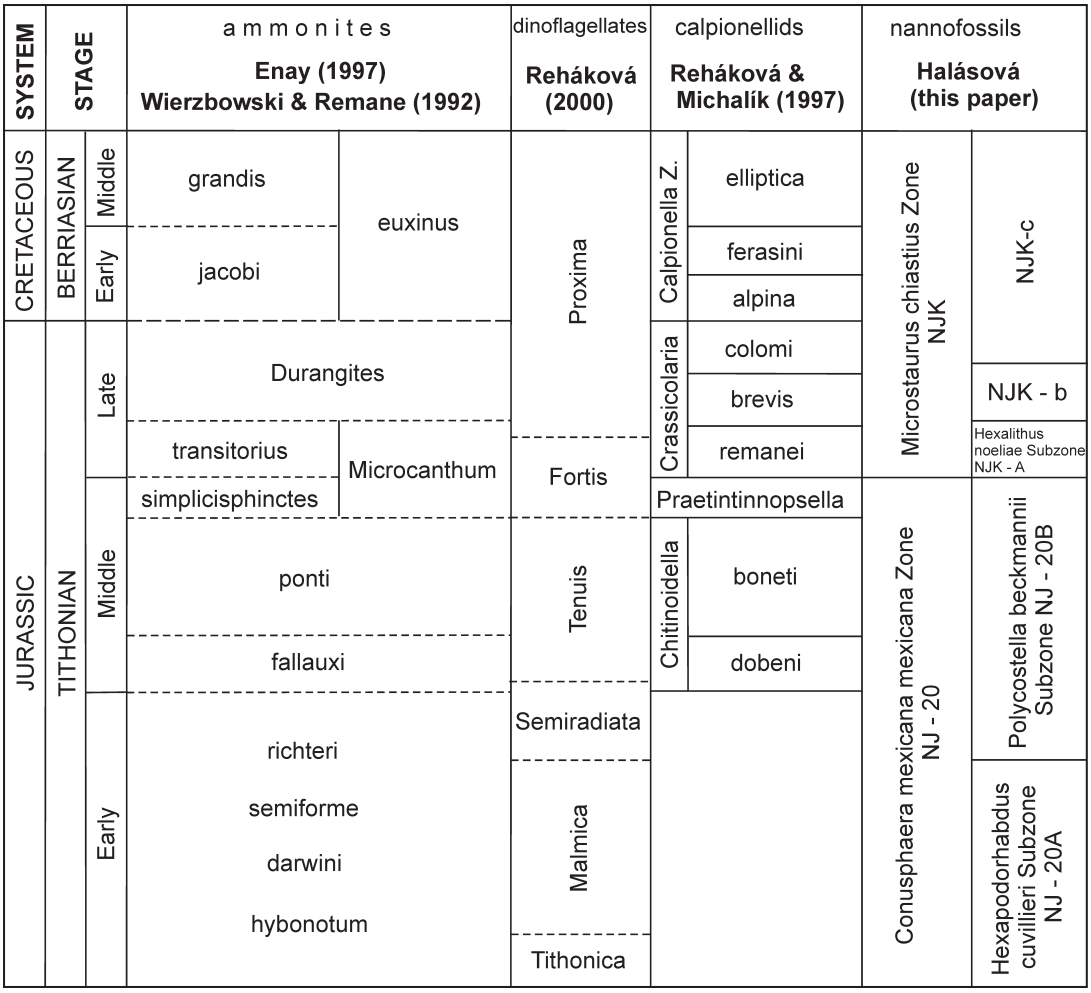

Fig. 11. Correlation scheme of the Jurassic/Cretaceous ammonite-, calcareous dinoflagellate-, calpionellid- and calcareous nannofossil biostratigraphic zonation.

Drawing the J/K boundary line in the Brodno sequence

As the West Carpathian J/K boundary sections are either condensed (Kutek & Wierzbowski 1966; Wierzbowski & Remane 1992), or extremely poor in ammonites, their biostratigraphy (Borza & Michalík 1986; Reháková 1995; Reháková & Michalík 1997a) was based mostly on calcareous microfossil (calpionellids and dinoflagellates) distribution. The standard Chitinoidella Zone is correlatable with the Polycostella beckmannii Subzone of the Conusphaera mexicana mexicana Zone. The Early/Middle Tithonian boundary in the Brodno succession could be situated at the FO of the nannolith *Polycostella beckmannii*. The Middle/Late Tithonian boundary was determined by the calpionellid standard Praetintinnopsella Zone which correlates with the FO of *Helenea chiastia* (in the Microstaurus chiastius Zone). The base of the Late Tithonian interval considering the standard Crassicollaria Zone was traced by the FO's of *Litraphidites carniolensis, Nannoconus infans*, *Nannoconus wintereri* and *Cruciellipsis cuvillieri* within the Microstaurus chiastius Zone.

The onset of the Alpina Subzone of standard Calpionella Zone which was identified with the J/K boundary by Borza & Michalík (1986), Remane et al. (1986), Reháková (1995), Reháková & Michalík (1997a), Lakova (1994) etc., occurs within this interval (Figs. 8, 9). Its base corresponds to the morphological change in *Calpionella alpina* loricas with a "relative explosion" of medium-sized sphaerical forms, as well as a sudden rapid decrease in their abundance (Remane et al. 1986). Several authors discussed complete disappearance or even extinction of crassicollarians (Tárdi-Filácz 1986; Reháková 2000a). The interval between the FO of *Nannoconus wintereri* co-occurring with small nannoconids, and the FO of *Nannoconus steinmanni minor*, interpreted as the Tithonian/Berriasian boundary interval (Bralower et al. 1989), was also recognized in the section studied (Fig. 9).

The detailed distribution of calcareous nannofossils, calpionellids and dinoflagellates has been correlated with the magnetostratigraphic polarity chrons, recognized in the Brodno section by Houša et al. (1996a and b). Two distinct fossil nannobioevents were recognized during the interval correlated with M20r to M20n Magnetozones: the dominance of nannoliths of *Polycostella beckmannii* (~calpionellid Chitinoidella Zone) and the appearance of the calcareous nannofossil association with *Helenea chiastia* (~calpionellid

Crassicollaria Zone). According to Houša et al. (1996a), the base of the standard Crassicollaria Zone in the Brodno section lies approximately in the middle of the M20n Magnetozone. According to our results, this limit should be traced higher; it aproximately coincides with the reverse Kysuca Subzone. Houša et al. (1999) correlated the base of the standard Calpionella Zone, namely the Jurassic/Cretaceous boundary with the middle part of the M19n Magnetochron (solution 2), between the C15A and C15B beds. Calpionellids studied in this work allowed us to correlate this boundary interval with levels close to the Brodno Subchron, namely the C24A–C25A beds (Figs. 7–9).

Paleoecology

As the most abundant taxa in the poorly diversified nannofossil association from the Brodno section are represented by dissolution-resistant forms, their fluctuation is only partially related to the original composition of the nannoplankton assemblage and it cannot be interpreted without taking into consideration the taphonomical and diagenetic changes.

The maxima of the nannofossil abundance are supplied by *Watznaueria barnesae* placoliths. Kessels et al. (2003) interpreted the Watznaueriaceae distribution pattern as an index of a low productive, oligotrophic setting with abundant K-selected cosmopolitan species. On the other hand, Lees et al. (2004), and Thomsen (1989) interpreted the bloom of this taxon as an indicator of a eutrophic environment with an opportunistic life strategy. Tremolada et al. (2006) supposed that *Watznaueria manivitae* represents an oligotrophic temperature-related taxon, while *Watznaueria britannica* was regarded as a mesotrophic or eutrophic taxon. The peak of the *Watznaueria* spp. in the Brodno sequence fits well the Late Tithonian cooling curve.

Another Late Tithonian peak of abundance (up to 20 %) in the Brodno succession refers to *Cyclagelosphaera margerelii* Pittet & Mattioli (2002) and Oliver et al. (2004) assumed that this taxon occupied an intermediate position in the trophic preference continuum between the more oligotrophic *Watznaueria manivitae* and the small-sized more eutrophic *Watznaueria britannica*. *Cyclagelosphaera margerelii* has been interpreted as an element of extremely abundant low-diversified neritic nannofloral assemblage from a lagoonal environment with marked salinity variations (Tremolada et al. 2006). Salinity variations should also have been responsible of thinning of the crassicollarian loricas around the J/K boundary (Reháková 2000a).

The most striking changes in the Brodno section concern the composition and abundance of three genera (*Conusphaera*, *Polycostella*, and *Nannoconus*). *Conusphaera* predominates in the late Lower Tithonian nannofossil association. The acme peak of *Polycostella* starts immediately later, at the beginning of the Middle Tithonian. The *Nannoconus* expansion is observed during the latest Tithonian (Fig. 5). Nannoconids were probably the most successfull group that adapted better to warmer and more stratified water masses. Erba (1994) supposed that the *Nannoconus* was a deep- (lower photic) dweller that flourished with a deep nutricline and marked oligotrophic surface waters. According to stable isotope data (Gröcke et al. 2003) this form flourished in warmer and possibly less nutrient-supplied surface waters than *Polycostella,* which proliferated in a relatively colder environment. The offset in abundance between *Nannoconus* spp., *Conusphaera* spp., and *Polycostella* spp. could result from biological competition in the same ecological niche (Bornemann et al. 2003) through significant changes in the temperature and nutrient availability during the J/K boundary. The gradual increase in thick calcifying nannoliths since the Middle Tithonian corresponds to the general enhancement of $CaCO_3$ and with the carbonate accumulation rates in western Tethys and middle Atlantic areas. Increased calcification of the nannoplankton was favoured by drier climate, atmospheric pCO_2 drop and more dynamic exchange of oligotrophic or alkaline surface oceanic waters (Bornemann, l. c.).

Occurrence of the first hyaline calpionellids (L94) can also be considered as a paleoenvironmental indicator. The Middle Tithonian microgranullar calpionellids were replaced by hyaline ones due to both the increase of the nutrient content (nannoplankton) and the high calcium carbonate saturation of sea-water (Reháková & Michalík 1997b). Two distinct morphological changes of hyaline calpionellids can be recognized during the Late Tithonian and Early Berriasian. The first one is characterized by the replacement of diversified crassicollarians association of the Remanei Subzone by the association in which small *Crassicollaria brevis* dominates. The second one was observed at the beginning of the Alpina Subzone where crassicollarians rapidly decreased in abundance and were completely replaced by small sphaerical *Calpionella alpina*. The abundance distribution of small calpionellids coincides with the intervals of higher abundances of nannoconids. Consider the *Nannoconus* as a deep- (lower photic) dweller, that flourished with a deep nutricline and marked oligotrophy of surface waters (Erba 1994), we can conclude that both microorganism groups inhabited similar environmental niches.

The stratigraphic and paleoecological potential of calcareous dinoflagellates has been discussed by Reháková (2000a,b). In the Brodno section, Lower Tithonian cysts show distinct change in abundance and composition. Orthopithonellids dominated in the Malmica Zone, but they were replaced by obliquipithonellids dominated by *Cadosina semiradiata semiradiata* in the Semiradiata Zone. Coinciding acme peaks of *Cadosina semiradiata semiradiata* and *Conusphaera* spp. represent probable indicators of warmer surface waters.

The data obtained indicate a sea water temperature in the range between 15.5–21.3 °C, when we used $\delta^{18}O_w$ –1.0 ‰ V-SMOW, deemed appropriate for the ice-free world of post-Jurassic times (Gröcke et al. 2003). These values fit the Kimmeridgian–Tithonian 14–21 °C temperature interval calculated by Gröcke et al. (l.c.), Price et al. (1997, 2000) for northern Tethys. However, this relative large (5–6 °C) temperature fluctuation seems to be unrealistic. A part of this apparent temperature fall could be attributed to the effect of surface-water salinity decrease (see also Tremolada et al. 2006, etc). The $\delta^{18}O$ indicates that the uppermost Tithonian deposits were formed during a relatively cold period (18.5 °C in average) temporally interrupted by warm episodes but overall arid rather than humid (Fig. 6). This is also documented by the monotonous $\delta^{13}C$ content and low con-

tents of organic carbon. Short term fluctuation of $\delta^{18}O$ values indicated temperature-, salinity changes and invasion of warm water (or stagnancy of cold water input) into the basin around the J/K boundary interval: this is documented by blooms and definitive expansion of nannoconids, accompanied by depletion of the calpionellid association.

Conclusions

The high-resolution quantitative analysis of calpionellids, dinoflagellates and calcareous nannofossil assemblages indicates major variations in their abundance and composition. Correlation of the calcareous microplankton distribution and stable isotope analyses was used in the characterization of the J/K boundary interval as well as in the reconstruction of the paleoceanography of this time.

The biostratigraphical study based on the distribution of calpionellids allowed us to distinguish the Dobeni Subzone of the Chitinoidella Zone in the Brodno sequence for the first time. The J/K boundary interval can be characterized by several calpionellid events — the onset, diversification, and extinction of chitinoidellids (Middle Tithonian); the onset, burst of diversification, and extinction of crassicollarians (Late Tithonian); and the onset of the monospecific *Calpionella alpina* association close to the J/K boundary.

The J/K boundary in the Brodno section is traced between the Crassicollaria and Calpionella Zone. This limit is defined by the morphological change of *Calpionella alpina* tests. The base of the Crassicollaria Zone is correlated with the reverse Kysuca Subzone, and the base of the standard Calpionella Zone is located just below the reverse Brodno Subzone.

The abundance peak of obliquipithonellid cysts in the Semiradiata Zone isochronous with flourishing *Conusphaera* spp. was used as the indicator of warmer surface waters.

For the first time, two nannozones: the Conusphaera mexicana mexicana and the Microstaurus chiastius Zones were distinguished in the Western Carpathians. Calcareous nannofossils from the lower half of the studied sequence are correlated with the Early to Middle Tithonian Conusphaera mexicana mexicana Zone (NJ-20). This zone comprises the Polycostella beckmannii Subzone; the latter consisting of the Hexalithus noeliae or NJK-A, NJK-b- and NJK-c Subzones.

Calcareous nannofossils show poorly diversified associations at the J/K boundary. The abundance of *Watznaueria* spp., *Cyclagelosphaera* spp., *Conusphaera* spp., and *Polycostella* spp. in the studied section is relatively high. Other nannofossils are rather rare. *Conusphaera* predominates in the Tithonian nannofossil assemblage (showing the Middle Tithonian peak). *Polycostella* increased in abundance during the Boneti Subzone of the Chitinoidella Zone. On the basis of the appearance of the *Polycostella beckmannii* nannoliths, the Early/Middle Tithonian boundary was located in the Polycostella beckmannii Subzone.

The Middle/Late Tithonian boundary was determined by the FO of the *Helenea chiastia* coccolith accompanied by the first small nannoconids. Small nannoconids appeared during the Late Tithonian and increased in abundance during the Berriasian. *Polycostella* group diminished in abundance towards the onset of the Crassicollaria Zone. The Late Tithonian interval was dated more precisely by the appearance of *Hexalithus noeliae* and *Litraphidites carniolensis* within the Microstaurus chiastius Zone.

From the point of view of nannofossil stratigraphy, the Tithonian/Berriasian boundary interval should be limited considering the FO of *Nannoconus wintereri* together with small nannoconids at the base, and the FO of *Nannoconus steinmanni minor* at the top. Evolution of nannofossil, calpionellid and dinoflagellate genera coincided with assumed paleoceanographical changes across the J/K boundary interval.

Stable isotope ($\delta^{18}O$, $\delta^{13}C$) analyses indicated a relatively cold period occasionally disturbed by warm episodes during the uppermost Tithonian. This is also documented by low contents of organic carbon. Near the J/K boundary the oxygen isotope values indicated temperature and salinity changes probably influenced by an invasion of warm water (or stagnancy of cold water input) into the basin resulting in nannoconid bloom episodes. Late Tithonian cooling was followed by temperature increase during the very end of the Tithonian and at the beginning of the Berriasian.

Acknowledgments: This is a contribution to the 506 IGCP UNESCO Project, APVV-0248-07, APVV-0280-07, APVV-0465-06, APVT 51-011305, and VEGA Grant Projects 6026, 2035 and 3178. We are grateful to Prof. Dr. Mabrouk Boughdiri, Dr. Michal Krobicki and Dr. J. Soták for critical reading of the text and for many inspiring comments.

References

Adatte T., Stinnesbeck W. & Remane J. 1994: The Jurassic–Cretaceous boundary in north-eastern Mexico. Confrontation and correlations by microfacies, clay minerals mineralogy, calpionellids and ammonites. *Géobios* 17, 37–56.

Allemann F., Catalano R., Farès F. & Remane J. 1971: Standard calpionellid zonation (Upper Tithonian–Valanginian) of the western Mediterranean Province. In: Farinacci A. (Ed.): *Proceedings, II Planktonic Conference*, Rome 1970, 2, 1337–1340.

Anderson T.F. & Arthur M.A. 1983: Stable isotope of oxygen and carbon and their application to sedimentologic and environmental problems. In: Arthur M.A., Anderson T.F., Kaplan I.R., Veizer J. & Land L.S. (Eds.): Stable isotopes in sedimentary geology. *Soc. Econ. Paleontol. Mineral. Short Course Note* 10, 1.1–1.151.

Andrusov D. 1938: Geological research of the inner Klippen Belt in Western Carpathians III. *Rozpr. Stát. Geol. Úst.* 9, 1–135 (in Czech).

Andrusov D. 1950: The Klippen Belt between Vlára River and Žilina. *Geol. Sbor. SAV* 1, 2–4, 288–292 (in Slovak).

Andrusov D. 1959: Geology of the Czechoslovakian Carpathians II. *Vydavateľstvo SAV*, Bratislava, 1–375 (in Slovak).

Birkenmajer K. 1977: Jurassic and Cretaceous lithostratigraphic units of the Pieniny Klippen Belt, Carpathians, Poland. *Stud. Geol. Pol.* 45, 1–158.

Bornemann A., Aschwer U. & Mutterlose J. 2003: The impact of calcareous nannofossils on the pelagic carbonate accumulation across the Jurassic–Cretaceous boundary interval. *Palaeogeogr. Palaeoclimatol. Palaeoecol.* 199, 187–228.

Borza K. 1969: Die Mikrofazies und Mikrofossilien des Oberjuras

und Unterkreide der Klippenzone der Westkarpaten. *Vydavateľstvo SAV*, Bratislava, 1–124.

Borza K. 1984: The Upper Jurassic–Lower Cretaceous parabiostratigraphic scale on the basis of Tintinninae, Cadosinidae, Stomiosphaeridae and other microfossils from the West Carpathians. *Geol. Zbor. Geol. Carpath.* 35, 2, 539–550.

Borza K. & Michalík J. 1986: Problems with delimitation of the Jurassic/Cretaceous boundary in the Western Carpathians. *Acta Geol. Hung.* 29, 1–2, 133–149.

Bralower T.J., Monechi S. & Thierstein H.R. 1989: Calcareous nannofossil zonation of the Jurassic-Cretaceous boundary interval and correlation with the geomagnetic polarity timescale. *Mar. Micropaleont.* 14, 153–235.

Channel J.E.T. & Grandesso P. 1987: A revised correlation of Mesozoic polarity chrons and calpionellid zones. *Earth Planet. Sci. Lett.* 85, 222–240.

Craig H. 1965: The measurement of oxygen isotope paleotemperatures. In: Tongiorgi E. (Ed.): Stable isotopes in oceanographic studies and paleotemperatures. *Consiglio Nazionale delle Richerche, Laboratorio di Geologia Nucleare,* Pisa, 161–182.

Dypvik H., Gudlaugsson S.T., Tsikalas F., Attrep M. Jr., Ferrell R.E. Jr., Krinsley D.H., Mørk A., Faleide J.I. & Nagy J. 1996: Mjølnir structure: An impact crater in the Barents Sea. *Geology* 24, 779–882.

Enay R. 1997: Le Jurassique Supérieur. In: Cariou E. & Hantzpergue (Eds.): Biostratigraphie du Jurassique Ouest-Européen et Méditerranéen. *Bull. Centre Rech. Elf Explor. Prod. Mém.* 17, 1–440.

Epstein S., Buchsbaum R., Lowenstam H.A. & Urey H.C. 1953: Revised carbonate-water isotopic temperature scale. *Geol. Soc. Amer. Bull.* 64, 1315–1326.

Erba E. 1994: Nannofossils and superplumes: the early Aptian "nannoconid crisis". *Paleoceanography* 9, 483–501.

Flandrin J., Schaer J.P., Enay R., Remane J., Rio M.M., Kubler M.B., Le Hégarat G., Mouterde R. & Thieuloy J.-P. 1975: Discussion génerale prélôiminaire au dépôt des motions. Colloque sur la limite Jurassique–Crétacé. *Mém. Bureau Recherches Géologiques et miniéres* 86, 386–393.

Gawlick H.-J. & Schlagintweit F. 2006: Berriasian drowning of the Plassen carbonate platform at the type-locality and its bearing on the early Eoalpine orogenic dynamics in the Northern Calcareous Alps (Austria). *Int. J. Earth Sci.* 95, 3, 451–462.

Grabowski J. & Pszczółkowski A. 2006: Magneto- and biostratigraphy of the Tithonian-Berriasian pelagic sediments in the Tatra Mountains (central Western Carpathians, Poland): sedimentary and rock magnetic changes at the Jurassic/Cretaceouas boundary. *Cretaceous Research* 27, 398–417.

Gradstein F.M., Agterberg F.S., Ogg J.G., Hardenbol J., VanVeen P., Thierry J. & Huang Z. 1995: A Triassic, Jurassic and Cretaceous time scale. In: Berggren W., Kent D.V., Aubry M.-P. & Hardenbol J. (Eds.): Geochronology, time scales and global stratigraphic correlation. *Soc. Sed. Geol., Spec. Publ.* 54, 95–126.

Gröcke D.R., Price G.D., Ruffell A.H., Mutterlose J. & Baraboshkin E. 2003: Isotopic evidence for Late Jurassic–Early Cretaceous climate change. *Palaeogeogr. Palaeoclimatol. Palaeoecol.* 202, 97–118.

Hay W.W., Migdisov A., Balukhovsky A.N., Wold Ch.N., Flögel S. & Söding E. 2006: Evaporites and the salinity of the ocean during the Phanerozoic: Implications for climate, ocean circulation and life. *Palaeogeogr. Palaeoclimatol. Palaeoecol.* 240, 1–2, 6, 3–46.

Hoedemaeker P.J. & Leereveld H. 1995: Biostratigraphy and sequence stratigraphy of the Berriasian–lowest Aptian (Lower Cretaceous) of the Rio Argos succession, Caravaca, SE Spain. *Cretaceous Research* 16, 195–230.

Hoedemaeker P.J., Company M.R., Aguirre Urreta M.B., Avram E., Bogdanova T.N., Bujtor L., Bulot L., Cecca F., Delanoy G., Ettachfini M., Memmi L., Owen H.G., Rawson P.F., Sandoval J., Tavera J.M., Theiuloy J.-P., Tovbina S.Z. & Vašíček Z. 1993: Ammonite zonation for the Lower Cretaceous of the Mediterranean region: basis for the stratigraphic correlation within IGCP Project 262. *Revista Española de Paleontología* 8, 117–120.

Houša V., Krs M., Krsová M. & Pruner P. 1996: Magnetostratigraphic and micropaleontological investigations along the Jurassic–Cretaceous boundary strata, Brodno near Žilina (Western Slovakia). *Geol. Carpathica* 47, 3, 135–151.

Houša V., Krs M., Krsová M., Man O., Pruner P. & Venhodová D. 1999: High-resolution magnetostratigraphy and micropaleontology across the J/K boundary strata at Brodno near Žilina, western Slovakia: summary of results. *Cretaceous Research* 20, 699–717.

Kessels K., Mutterlose J. & Ruffell A. 2003: Calcareous nannofossils from late Jurassic sediments of the Volga Basin (Russian Platform): evidence for productivity-controlled black shale deposition. *Int. J. Earth Sci.* 92, 5, 743–757.

Koeberl C., Armstrong R.A. & Reymold W.U. 1997: Morokweng, South Africa: A large impact structure of Jurassic-Cretaceous boundary age. *Geology* 25, 731–734.

Kutek J. & Wierzbowski A. 1986: A new account on the Upper Jurassic stratigraphy and ammonites of the Czorsztyn succession, Pieniny Klippen Belt, Poland. *Acta Geol. Pol.* 36, 4, 289–316.

Lakova I. 1994: Numerical criteria of precise delimitation of the calpionellid Crassicollaria and Calpionella zones in relation to the Jurassic/Cretaceous system boundary. *Geol. Balcanica* 24, 6, 23–30.

Leckie M.R., Bralower T.J. & Cashman R. 2002: Ocean anoxic events and plankton evolution. Biotic response to tectonic forcing during Cretaceous. *Paleoceanography* 17, 3, 1041, doi: 10.1029/2001PA000623.

Lees J.A., Bown P.R., Young J.R. & Riding J.B. 2004: Evidence for annual records of phytoplankton productivity in the Kimmeridge Clay Formation coccolith stone bands (Upper Jurassic, Dorset, UK). *Mar. Micropaleont.* 52, 29–49.

Lini A., Weissert H. & Erba E. 1992: The Valanginian isotope event: a first episode of greenhouse climate conditions during the Cretaceous. *Terra Nova* 4, 374–384.

Lowrie W. & Channel J.E.T. 1983: Magnetostratigraphy of the Jurassic–Cretaceous boundary in the maiolica limestone (Umbria, Italy). *Geology* 12, 44–47.

Mahoney J.J., Duncan R.A., Tejada M.L.G., Sager W.W. & Bralower T.J. 2005: Jurassic-Cretaceous boundary age and mid-ocean-ridge-type mantle source for Shatsky Ridge. *Geology* 33, 3, 185–188.

Márton E. 1986: The problems of correlation between magnetozones and calpionellid zones in Late Jurassic–Early Cretaceous sections. *Acta Geol. Hung.* 29, 125–131.

Michalík J. 2007: Rock record and microfacies indicators of the Jurassic/Lower Cretaceous pull-apart development of the Zliechov Basin, central Western Carpathians. *Geol. Carpathica* 58, 5, 443–453.

Michalík J., Reháková D. & Peterčáková M. 1990: To the stratigraphy of Jurassic–Cretaceous boundary beds in the Kysuca sequence of the West Carpathian Klippen belt Brodno section near Žilina. *Zemní Plyn Nafta* 9b, 57–71.

Michalík J., Reháková D., Hladíková J. & Lintnerová O. 1995: Lithological and biological indicators of orbital changes in Tithonian and Lower Cretaceous sequences, Western Carpathians, Slovakia. *Geol. Carpathica* 46, 3, 161–174.

Michalík J., Soták J., Lintnerová O., Halásová E., Bąk M., Skupien P. & Boorová D. 2008: The stratigraphic and palaeoenvironmental setting of Aptian OAE black shale deposits in the Pieniny Klippen Belt, Slovak Western Carpathians. *Cretaceous*

Research 29, 871–892.

Mutterlose J. & Kessels K. 2000: Early Cretaceous calcareous nannofossils from high latitudes: implications for palaeobiogeography and palaeoclimate. *Palaeogeogr. Palaeoclimatol. Palaeoecol.* 160, 347–372.

Ogg J.G. & Lowrie W. 1986: Magnetostratigraphy of the Jurassic–Cretaceous boundary. *Geology* 14, 547–550.

Ogg J.G., Hasenyager R.W., Wimbledon W.A., Channel J.E.T. & Bralower T.J. 1991: Magnetostratigraphy of the Jurassic–Cretaceous boundary interval — Tethyan and English faunal realms. *Cretaceous Research* 12, 455–482.

Oliver N., Pittet B. & Mattioli E. 2004: Paleoenviromental control on sponge reefs and contemporaneous deep-shelf marl-limestone deposition (Late Oxfordian, southern Germany). *Paleogeogr. Paleoclimatol. Paleoecol.* 212, 233–263.

Olóriz F. & Tavera J.M. 1990: The Jurassic–Cretaceous boundary in Southern Spain. Some eco-stratigraphical considerations. *Acad. Sci. U.S.S.R.* 699, 64–78.

Olóriz F., Caracuel J.E., Marques B. & Rodriguez-Tovar F.J. 1995: Asociaciones des Tintinnoides en facies ammonitico rosso de la Sierra Norte (Mallorca). *Rev. Española Paleont., Número Homenaje al Dr. Guillermo Colom*, 777–793.

Pittet B. & Mattioli E. 2002: The carbonate signal and calcareous nannofossil distribution in an Upper Jurassic section (Balingen–Thieringen, Late Oxfordian, southern Germany). *Paleogeogr. Paleoclimatol. Paleoecol.* 179, 71–96.

Pop G. 1997: Révision systématique des chitinoidelles tithoniennes des Carpathes Méridionales (Roumanie). *Compte Rendus Acad. Sci.*, *Série II a*, Paris 342, 931–938.

Price G.D. & Sellwood B.W. 1997: 'Warm' palaeotemperatures from high Late Jurassic palaeolatitudes (Falkland Plateau): Ecological, environmental or diagenetic controls? *Paleogeogr. Paleoclimatol. Paleoecol.* 129, 315–327.

Price G.D., Valdes P.J. & Selwood B.W. 1998: A comparison of GCM simulated Cretaceous "greenhouse" and "icehouse" climate: implication for the sedimentary record. *Paleogeogr. Paleoclimatol. Paleoecol.* 142, 123–138.

Price G.D., Ruffell A.H., Jones C.E., Kalin R.M. & Mutterlose J. 2000: Isotopic evidence for temperature variation during the Early Cretaceous (late Ryazanian–mid-Hauterivian). *J. Geol. Soc. London* 157, 335–343.

Pszczółkowski A., García Delgado D. & González Gil S. 2005: Calpionellid and nannoconid stratigraphy and microfacies of limestones at the Tithonian–Berriasian boundary in the Sierra del Infierno (Western Cuba). *Ann. Soc. Geol. Pol.* 75, 1–16.

Reháková D. 1995: New data on calpionellid distribution in the Upper Jurassic/Lower Cretaceous formations (Western Carpathians). *Miner. Slovaca* 27, 308–318 (in Slovak).

Reháková D. 2000a: Calcareous dinoflagellate and calpionellid bioevents versus sea-level fluctuations recorded in the West-Carpathian (Late Jurassic/Early Cretaceous) pelagic environments. *Geol. Carpathica* 51, 4, 229–243.

Reháková D. 2000b: Evolution and distribution of the Late Jurassic and Early Cretaceous calcareous dinoflagellates recorded in the Western Carpathian pelagic carbonate facies. *Miner. Slovaca* 32, 79–88.

Reháková D. 2002: *Chitinoidella* Trejo, 1975 in Middle Tithonian carbonate pelagic sequences of the West Carpathian Tethyan area. *Geol. Carpathica* 53, 6, 396–379.

Reháková D. & Michalík J. 1992: Correlation of Jurassic–Cretaceous boundary beds in West Carpathian profiles. *Földt. Közl.* 122, 1, 51–66.

Reháková D. & Michalík J. 1994: Abundance and distribution of Late Jurassic–Early Cretaceous microplankton in Western Carpathians. *Géobios* 27, 2, 135–156.

Reháková D. & Michalík J. 1997a: Evolution and distribution of calpionellids — the most characteristic constituents of Lower Cretaceous Tethyan microplankton. *Cretaceous Research* 18, 493–504.

Reháková D. & Michalík J. 1997b: Calpionellid associations versus Late Jurassic and Early Cretaceous sea level fluctuations. *Miner. Slovaca* 29, 4–5, 306–307.

Řehánek J. 1992: Valuable species of cadosinids and stomiosphaerids for determination of the Jurassic–Cretaceous boundary (vertical distribution, biozonation). *Scr. Univ. Brun., Geol.* 22, 117–122.

Remane J. 1971: Les calpionelles, protozoaires planctoniques des mers mésogéennes de l'Epoque Secondaire. *Ann. Guébhard* 47, 1–25.

Remane J. 1986: Calpionellids and the Jurassic-Cretaceous boundary. *Acta Geol. Hung.* 29, 15–26.

Remane J. 1991: The Jurassic–Cretaceous boundary: problems of definition and procedure. *Cretaceous Research* 12, 447–453.

Remane J., Borza K., Nagy I., Bakalova-Ivanova D., Knauer J., Pop G. & Tardi-Filácz E. 1986: Agreement on the subdivision of the standard calpionellid zones defined at the 2nd Planktonic Conference, Roma 1970. *Acta Geol. Hung.* 29, 5–14.

Roth P.H., Medd A.W. & Watkins D.K. 1983: Jurassic calcareous nannofossil zonation, an overview with new evidence from Deep Sea Drilling Project Site 534A. In: Sheridan R.E. & Gradstein F.M. et al. (Eds.): *Initial Reports DSDP* 76, Washington 573–579.

Samuel O., Gašparíková V. & Ondrejíčková A. 1988: Microbiostratigraphic correlation of the Lower and Middle Cretaceous sequences of the western part of the Klippen Belt. *MS, D. Štúr's Geol. Inst.*, Bratislava, 1–60.

Scheibner E. 1961: Mesozoic of the Pieniny Klippen Belt. In: Excursion guide of 12th Congress of Czecho-Slovakian Mineralogical and Geological Association, Ser. B — Mesozoic. 71–79 (in Slovak).

Scheibner E. 1962: Some new knowledge from Klippen Belt in Slovakia. *Geol. Práce*, *Spr.* 62, 233–238.

Scheibner E. 1967: Carpathian Klippen Belt. In: Buday T. et al. (Eds.): Regional geology of ČSSR. Western Carpathians II, 2. *Academia* Praha, 7–105.

Scheibner E. & Scheibnerová V. 1969: Type profile of the Kysuca Sequence (unit), (Pieniny Klippen Belt, Carpathians). *Věst. Ústř. Úst. Geol.* 44, 339–349.

Schlager W. 2005: Carbonate sedimentology and sequence stratigraphy. *SEPM Concepts in Sedimentology and Paleontology* 8, 1–200.

Schnyder J., Gorin G., Soussi M., Baudin F. & Deconinck J.F. 2005: Enregistrement de la variation climatique au passage Jurassique/Crétacé sur la marge sud de la Téthys: mineralogie des argiles et palynofacies de la coupe du Jebel Meloussi (Tunisie Centrale, Formation Sidi Kralif). *Bull. Soc. Géol. France* 176, 2, 171–182.

Schnyder J., Ruffel A., Deconink J.F. & Baudin F. 2006: Conjunctive use of spectral gama-ray logs and clay mineralogy in defining late Jurassic-early Cretaceous palaeoclimate. *Paleogeogr. Paleoclimatol. Paleoecol.* 229, 303–320.

Tárdi-Filácz E. 1986: Investigation of Calpionellidae remnants from the Tithonian–Berriasian basic profiles of Tata and Sümeg. *Acta Geol. Hung.* 29, 37–44.

Tavera J.M., Aguado R., Company M. & Olóriz F. 1994: Integrated biostratigraphy of the Durangites and Jacobi Zones (J/K boundary) at the Puerto Escaño section in Southern Spain (province of Cordoba). *Geobios*, *M.S.* 17, 469–476.

Thomsen E. 1989: Seasonal variation in boreal Early Cretaceous calcareous nannofossils. *Mar. Micropaleont.* 15, 123–152.

Tremolada F., Bornemann A., Bralower T., Koeberl C. & van de Schootbrugge B. 2006: Paleoceanographic changes across the Jurassic/Cretaceous boundary: the calcareous phytoplankton

response. *Earth Planet. Sci. Lett.* 241, 361–371.

Vašíček Z., Reháková D., Michalík J., Peterčáková M. & Halásová E. 1992: Ammonites, aptychi, nanno-and microplankton from the Lower Cretaceous Pieniny Formation in the "Kysuca Gate" near Žilina (Western Carpathian Klippen Belt, Kysuca Unit). *Západ. Karpaty*, *Paleont.* 16, 43–57.

Weissert H. & Channell J.E.T. 1989: Tethyan carbonate carbon isotope stratigraphy across the Jurassic-Cretaceous boundary: an indicator of decelerated global carbon cycling? *Paleoceanography* 4, 483–494.

Weissert H. & Lini A. 1991: Ice Age interludes during the time of Cretaceous Greenhouse Climate? In: Müller D.W., McKenzie J.A. & Weissert H. (Eds.): "Controversies in modern geology". *Academic Press*, 173–191.

Weissert H. & Mohr H. 1996: Late Jurassic climate and its impact on carbon cycling. *Palaeogeogr. Palaeoecol. Palaeoclimatol.* 122, 27–43.

Wierzbowski A. & Remane J. 1992: The ammonite and calpionellid stratigraphy of the Berriasian and lowermost Valanginian in the Pieniny Klippen Belt (Carpathian, Poland). *Eclogae Geol. Helv.* 85, 3, 871–891.

Zakharov V.A., Bown P. & Rawson F. 1996: The Berriasian Stage and the Jurassic-Cretaceous Boundary. *Bull. Inst. Roy. Sci. Natur. Belg, Sci. Terre* 66, suppl., 7–10.